MARTIN MARIETTA ENERGY SYSTEMS LIBRARIES
3 4456 0361391 7

151

CENTRAL RESEARCH LIBRARY
DOCUMENT COLLECTION

ORNL-2742
UC-40 - Radiation Effects on Materials

A STUDY OF THE EFFECTS OF FISSION FRAGMENT RECOILS ON THE OXIDATION OF ZIRCONIUM

W. C. Yee

CENTRAL RESEARCH LIBRARY
DOCUMENT COLLECTION
LIBRARY LOAN COPY
DO NOT TRANSFER TO ANOTHER PERSON
If you wish someone else to see this document, send in name with document and the library will arrange a loan.

OAK RIDGE NATIONAL LABORATORY
operated by
UNION CARBIDE CORPORATION
for the
U.S. ATOMIC ENERGY COMMISSION

Printed in USA. Price $2.50. Available from the
Office of Technical Services
Department of Commerce
Washington 25, D.C.

LEGAL NOTICE

This report was prepared as an account of Government sponsored work. Neither the United States, nor the Commission, nor any person acting on behalf of the Commission:

A. Makes any warranty or representation, expressed or implied, with respect to the accuracy, completeness, or usefulness of the information contained in this report, or that the use of any information, apparatus, method, or process disclosed in this report may not infringe privately owned rights; or

B. Assumes any liabilities with respect to the use of, or for damages resulting from the use of any information, apparatus, method, or process disclosed in this report.

As used in the above, "person acting on behalf of the Commission" includes any employee or contractor of the Commission, or employee of such contractor, to the extent that such employee or contractor of the Commission, or employee of such contractor prepares, disseminates, or provides access to, any information pursuant to his employment or contract with the Commission, or his employment with such contractor.

ORNL-2742

Contract No. W-7405-eng-26

Reactor Experimental Engineering Division

and

Metallurgy Division

A STUDY OF THE EFFECTS OF FISSION FRAGMENT RECOILS ON THE OXIDATION OF ZIRCONIUM

William C. Yee

DATE ISSUED

APR 29 1960

Submitted as a Thesis to the Graduate Council of the University of Tennessee in partial fulfillment of the requirements for the degree of Master of Science

OAK RIDGE NATIONAL LABORATORY
Oak Ridge, Tennessee
operated by
UNION CARBIDE CORPORATION
for the
U.S. ATOMIC ENERGY COMMISSION

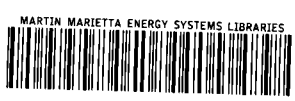

3 4456 0361391 7

ACKNOWLEDGEMENT

It is the pleasant duty of this author to record his appreciation to those people whose contributions aided immensely in the completion of the work presented.

The author is most indebted to Dr. G. H. Jenks who suggested the problem, guided him through the difficulties inherent to the problem and its interpretation, and criticized the prepared manuscript. The author is also most grateful to Dr. E. E. Stansbury who furnished the entire conceptual design for this experiment and aided greatly in the preparation of this manuscript by his criticisms and suggestions. The author acknowledges the kindness of Mr. E. G. Bohlmann for his administrative approval of the pursuit of this problem and the initial encouragement given to this writer by Dr. C. H. Secoy in providing a basis whereby it would be possible to do this work at the Oak Ridge National Laboratory.

Special thanks are due to the following personnel of ORNL for their invaluable contributions to this work: J. V. Cathcart for his suggestions on the techniques of studying the specimen surfaces both by optical and electron microscopy and for his interpretation of all these results; M. L. Picklesimer for the reported optical microscopy study of the surfaces of the specimens both under normal illumination and under polarized light and his interpretation of the results of the study; F. W. Young, Jr. for his helpful comments on the correlation of the

experimental data; E. L. Long, Jr. and W. H. Bridges and their group including J. T. Houston and C. D. Mathes for doing the detailed optical and electron microscopy studies on all of the specimen surfaces and for all of the laborious photography that is intrinsic to these types of studies; A. R. Olsen for his direct supervision of all of the techniques used in the remote disassembly of each radioactive experiment and his group including B. W. McCollum, leader, and C. M. Fitzpatrick, W. J. Schill, and W. H. Smith, Jr. for all of the work in disassembling remotely each of these experiments; G. W. Leddicotte, S. A. Reynolds, and J. S. Eldridge for their activation analyses of all of the irradiated zirconium specimens; C. D. Cagle and W. R. Casto for their helpful suggestions in the design of an in-pile experiment; R. J. Beaver, D. T. Bourgette, C. F. Leitten, Jr., and G. M. Slaughter for the method of preparation and actual fabrication of the fission fragment recoil source employed in this experiment and for the copper brazing technique used to bond this source to a cooling unit; C. A. Mossman and P. P. Williams for their design and construction of the instrumentation for this experiment; T. L. Trent and his group including C. L. Terry for the detailed design of the autoclave unit employed; and W. A. Blevins, D. L. Holcomb, and A. B. Keeney for their supervision in fabricating the components of the especially designed autoclaves. The author also wishes to thank W. W. Harris of the Technical Division at the Oak Ridge Gaseous Diffusion Plant for his electron microscopy work on the metal specimens.

For their efforts in attempting to develop a suitable fission fragment recoil source, the author is indebted to the following members

of ORNL: D. T. Jones for his suggestions and his aid in attempting to obtain a metallic bond between a ternary uranium alloy (5 ^{w}/o Zr - 1$\frac{1}{2}$ ^{w}/o Nb) to aluminum bronze; J. H. Erwin and his group for the actual fabrication attempts to bond this ternary alloy to the aluminum bronze; and A. J. Taylor and his group for fabricating and testing a variety of uranium compounds in powder compact form to see if any of these forms of uranium would make a suitable source. Also the author is grateful to J. E. Draley, F. L. Yagee, and R. E. Macherey of the Argonne National Laboratory for furnishing research quantities of the ternary uranium alloy for experimental use.

The author desires to express his gratitude to D. K. Holmes, H. W. Schmitt, W. L. Carter, J. E. Baker, A. C. Downing, and N. M. Dismuke for their assistance in developing the mathematical relationships needed to both design the experiment and to interpret the results of the experiment.

Direct assistance and/or information was also obtained from other members of the ORNL staff. They included: J. W. Boyle and P. S. Rudolph of the Chemistry Division; T. E. Willmarth, U. Koskela and R. L. Sherman of the Analytical Chemistry Division; the foremen T. B. Nixon, C. McBee, E. D. Lance, L. P. Jernigan and R. D. Hulen and their respective operating personnel of the Reactor Operations Department; and R. A. Lorenz, V. A. DeCarlo, and V. R. Bullington of the Solution Radiation Corrosion Section of REED Division. The author is grateful for their collective efforts on his behalf.

The author is truly indebted to Miss Mildred Gregg, Secretary of the Solution Radiation Corrosion Section, for her efficient and superb preparation of this manuscript.

To the Graphic Arts Department, the author expresses his thanks for the splendid art work contained in this report.

And finally, the author is grateful to the Union Carbide Nuclear Company for permission to participate in the employee educational assistance program.

TABLE OF CONTENTS

LIST OF TABLES

LIST OF FIGURES

FIGURE PAGE

FIGURE PAGE

CHAPTER I

SUMMARY

The objective of this series of experiments was to study the effects of fission fragment recoils on the corrosion of zirconium in an oxygen atmosphere at 250°C.

Each of the experiments was conducted in an especially designed autoclave unit which contained four zirconium specimens and a source of fission fragments as required. Four runs — three of them with a source — were conducted in Hole 16 of the Graphite Reactor at ORNL where the maximum thermal neutron flux is 8.5×10^{11} neutrons/cm^2/second at a power of 3.5 Mw.

The experiment was designed to provide for oxidation of specimens under the following conditions: (1) reactor radiations including fission fragment recoils, (2) reactor radiation in the absence of fission fragment recoils, and (3) no radiation. All other variables were maintained as constant as possible. To observe differences due to fission fragments alone, two of the four zirconium specimens contained in each of the autoclave units were located such that one surface of each specimen could be exposed to fission fragment recoils. These were designated as the test specimens. The other two specimens in the autoclave, designated as the control specimens, were exposed to the same neutron flux as the test specimens but were not subject to fission fragment recoil bombardment. To provide a basis for interpreting the data of the in-pile experiments, another set of specimens was exposed

out-of-pile.

The test specimens were maintained at 250°C while the control specimens operated at 265°C. This temperature difference was due to the inherent features of the design of the experiment.

The results of the analyses made on the zirconium specimens indicated that fission fragment recoils did physically affect the oxide film. According to a microscopic study of the specimens, those surfaces that were exposed to recoils showed significant differences when viewed under polarized light from those which had not been exposed to recoils. Low angle electron diffraction patterns of the surface of a specimen exposed to fission fragment recoils showed very diffuse rings while the patterns from the surface that was in a neutron flux only showed a relatively large number of spotty rings. A surface topography study of the specimens using the electron microscope showed that the majority of those surfaces exposed to recoils had a rough, mottled surface while the surfaces exposed to a neutron flux were, in general, much smoother.

These observations may be interpreted as the fission fragment recoils affecting the oxide film in either or both of two ways: (1) the oxide had undergone a phase transformation and/or (2) the oxide had developed a fine particle size with random orientation. The possibility of a phase transformation was indicated by the observed significant change in optical anisotropy under polarized light with the microscope employed. The diffuse ring pattern as revealed by low angle electron

diffraction suggested that the oxide film had developed a fine particle size with random orientation. It is possible for an oxide of this fine particle size to exhibit the observed change in optical anisotropy without the necessity of a phase transformation.

The number of experiments performed was insufficient to permit conclusive interpretation of the weight changes. The limited data indicated that there was a greater weight gain in the zirconium specimens oxidized in-pile than those oxidized out-of-pile. If this observation can be considered significant, the effect could be attributed to either an alteration in the chemical nature of the gas environment surrounding the specimens or due to the fast neutron flux and fission fragment recoils directly on the specimens or both.

CHAPTER II

INTRODUCTION

Numerous experiments have been performed during the past several years to determine the effects of reactor radiation on the corrosion of reactor components using aqueous homogeneous reactor fuel systems. The metals from which the components of such reactors are built — various alloys of zirconium, assorted types of stainless steel and titanium metal — have been irradiated under a variety of conditions. The present research has developed from such studies in uranyl sulfate solutions, the fuel of the ORNL Homogeneous Reactor. The portion of the reactor in which the nuclear chain reaction proceeds to produce power is called the core and is made of Zircaloy-2. Consequently many studies have been made with this metal subjected to radiation conditions in environments similar to those within the reactor core. The over-all operating temperature range within the core region is 250-300°C.

It has been shown that under radiation the corrosion rate of Zircaloy-2 and zirconium in uranyl sulfate solutions is appreciably greater than in similar control experiments run in the absence of radiation. Jenks[1] has very adequately summarized the results of these experiments to date.

Several mechanisms have been considered to explain this increase in corrosion rate. These involve the effects of irradiation on (1) the dilute uranyl sulfate solution and (2) the metal and/or its oxide film.

For aqueous solutions, it has been reported[2] that the initial products of irradiation are hydrogen peroxide and the free radicals H and OH. These provide a possible means of influencing the corrosive properties of the liquid; however, Jenks[3] has reported that the results of radiation studies of Zircaloy-2 and zirconium in uranyl sulfate solutions to date have indicated that the increased corrosion rate is not directly due to changes in the solution itself.

The alternate interpretation advanced[4] for the observed increase in corrosion rate of Zircaloy-2 and zirconium under radiation is that the damage is due to heavy nuclear particle bombardment on the metal and/or its protective oxide film. This loss in the protective nature of the oxide film may be due to its conversion to a different phase. Wittels and Sherrill[5] have reported that upon exposure of bulk monoclinic ZrO_2 to an integrated fast neutron flux of approximately 10^{20} nvt_f at approximately 100°C, evidence was found of an oxide phase transformation to the cubic structure at uranium impurity sites[6] which were detected in the oxide. This would suggest that heavy nuclear particles such as fission fragment recoils were responsible for this change to the cubic structure since the recoils produced from fissioning of uranium have very short path lengths in a solid — in the order of 1-10 microns. Under normal conditions, the cubic ZrO_2 is stable only above 1900°C.[7]

Consideration may be given also to the consequences of fission fragment recoils on the metal itself. This model proposes[4] that the

recoils increase the activity of the metal by the production of defects within the metal. For zirconium, in particular, it has been suggested[8] that the normal oxidation reaction occurs at the metal-oxide interface. Because of these defects, the metal and hence the interface can become more reactive.

Since the study of the aqueous corrosion of zirconium under irradiation involves the resolution of several variables, it was thought that experimental data on the effects of heavy nuclear particles on zirconium corrosion in oxygen would be of aid in interpreting the aqueous radiation corrosion results. Specifically, this information might be helpful in separating the effects in the oxide and/or metal due to radiation per se from those due to changes in the aqueous environment.

Thus the present series of experiments, as envisioned, involved the exposure of zirconium specimens to fission fragment recoils in an oxygen environment. For purposes of comparison, it was essential to design the experiment to provide zirconium control specimens which would be in the same reactor radiation intensities as the former specimens but would not be subject to fission fragment recoil bombardment.

Cognizance was given to the chemical nature of the gas in the presence of high energy nuclear particles such as β and γ-rays. This factor could have influenced the corrosion of the zirconium specimens and so must be considered in the interpretation of the experimental results. However it was felt that the effects of reactor radiations and heavy nuclear particles on an oxygen environment would be less

complex than that in a liquid media. Also, it was possible to arrange a relatively simple experimental system since the pressure problems which are encountered with aqueous media exposed to reactor radiations were not present.

CHAPTER III

THEORY

The ordinary reaction of zirconium with oxygen, at temperatures up to 400°C, has been characterized as one in which there is an initial rapid reaction followed by a decreasing rate as the oxide film thickens. The oxide layer is reported to adhere very tenaciously to the base metal and is reported by some investigators to be of the monoclinic[9] form. Other investigators have reported the cubic[10] and tetragonal[11] forms. It has been suggested[8] that the basic mechanism of zirconium oxidation involves oxygen diffusion through the oxide film via anion vacancies to the metal-oxide interface where the reaction proceeds. It is probable that anything which changes the oxide characteristics or the activity of the metal could affect the rate of oxidation.

Since the results of aqueous corrosion of Zircaloy-2 and zirconium under radiation suggest that the observed increase in corrosion rate is primarily due to the influence of heavy nuclear particles on the metal and/or its oxide film, only these types of disturbances will be discussed here.

Jenks[4] has recently postulated a model by which it is possible to interpret the effects of radiation on the corrosion of Zircaloy-2 and zirconium in an aqueous media. The model states that heavy nuclear particles such as fission fragment recoils produce defects of an unspecified nature in the metal and/or its oxide film. The net increase in

defects is proportional to the difference between the rate of formation of defects as determined by the radiation intensity at the solid and the rate of removal of defects which is a function of both radiation and thermal annealing factors. A steady-state postulated concentration of defects is reached when the rate of formation of defects equals the rate of removal of defects. For the oxide film, these defects are considered responsible for the film changing from a protective to a non-protective form and eventually scaling. For the metal, it is postulated that recoils increase the activity of the metal through production of displaced atoms[12] in the metal lattice which become significant in accelerating the reaction at the metal-oxide interface.

The extent of this radiation-induced increase in corrosion rate has been reported by Jenks[13] to be a function of the power density as determined by the effective concentration of enriched uranium in the proximity of the metal wall. This effective concentration may be simply that of the uranyl sulfate solution near the wall or may be due to a large extent to uranium being adsorbed on the wall.

CHAPTER IV

METHOD

A relatively simple method was employed for the present study. The experiments were performed in an autoclave unit which contained zirconium specimens located close to a source of fission fragment recoils which bombarded the specimens. These specimens were held at 250°C in an oxygen environment.

In addition to the zirconium samples which were exposed to fission fragments, provisions were made to insert control samples into the autoclave unit such that they were exposed to all of the corresponding nuclear conditions of the other samples with the one exception of the fission fragment recoils. Thus it would be possible to better isolate the effects due to recoils alone.

Autoclave units inserted in-pile for one week were filled with oxygen once, and the system isolated prior to exposure. Experiments run for two weeks were provided with a system whereby oxygen was added daily.

The fission fragment recoil source finally adopted was a uranium dioxide-stainless steel unit fabricated by powder metallurgy techniques. Although this source may have tolerated the temperature environment of the experiment, the heat generated by uranium fission, when in a neutron flux, had to be removed. To provide adequate cooling, the source was bonded by copper brazing to a cooling unit through which water was continuously circulated. This assembly performed satisfactorily for all

the experiments. In a temperature environment ranging from 250 to 300°C both in and out of the reactor flux, the disc was maintained below 65°C.

At the conclusion of each run, the zirconium specimens were separated from the experimental unit using remote techniques. Measurements of weight changes of the specimens were made. The surfaces of the specimens were studied subsequently by visual examination, by microscopic examination both at low and high magnification under normal illumination and polarized light, and by utilizing the electron microscope to obtain low angle electron diffraction patterns of the surfaces and to survey the topography of carbon replicas of the surfaces.

CHAPTER V

DESCRIPTION OF EQUIPMENT

The design criteria for any experiment which is to be exposed to a neutron flux within a research reactor are quite demanding. Two requirements were particularly significant in this experiment: they were compactness of over-all design and ease of disassembly. Compactness was necessary to accommodate the limits imposed by the geometry and size of the particular hole of the reactor in which the experiment was to be placed. Because of the radioactivity of an experiment at the end of an exposure, it was necessary to disassemble the unit using remote techniques in an adequately shielded dismantling cell. Therefore it was desirable to incorporate into the design a simple method of removing the zirconium specimens from the rest of the unit. Since it was anticipated that the specimen weight changes would be relatively small, any gross mechanical manipulation could be a source of error.

The actual equipment employed attempted to embrace the above design objectives. The experiments were carried out in autoclave units fabricated of aluminum bronze and stainless steel. There were three main components to each unit: (1) a water cooled stainless steel holder containing the fission fragment recoil source, (2) a heated, hollow, cylindrical body, and (3) a specimen holder. The source was placed in one end of the hollow cylinder. Inserted at the other end was the specimen holder containing the properly located zirconium specimens. The parts of the autoclave were assembled with threaded joints using

copper gaskets as seals. Prior to irradiation, each experimental assembly was sheathed in an aluminum can to contain any radioactive particle contaminants that might originate from the components of the unit. Figure 1 is a schematic diagram which locates the specimens and source within the autoclave unit. Photographs of the components of the autoclave and the assembled unit are shown in Figures 2 and 3, respectively.

Fission Fragment Recoil Source

The mechanics of preparing a suitable fission fragment recoil source and bonding it to the cooler unit became quite involved. Approaches considered before finding a satisfactory solution to the problem are mentioned briefly in Appendix A. The best suited fission source was prepared[14] by sintering a carefully blended mixture of uranium dioxide and pre-alloyed stainless steel powders. This material was clad in stainless steel, hot rolled to the desired thickness and one steel surface milled away. This bared the sintered material on one side. Circular discs were stamped from this strip of metal. Each disc was attached to a cooling unit by copper brazing. A schematic diagram of the source and the cooling unit is shown in Figure 4. Figure 5 is a photograph of the entire assembly.

Enriched uranium dioxide powder was employed (93.17% U^{235}) and constituted 36% by weight, as UO_2, of the binary mixture. The actual density of this sintered material was 8.35 g/cc and represented greater

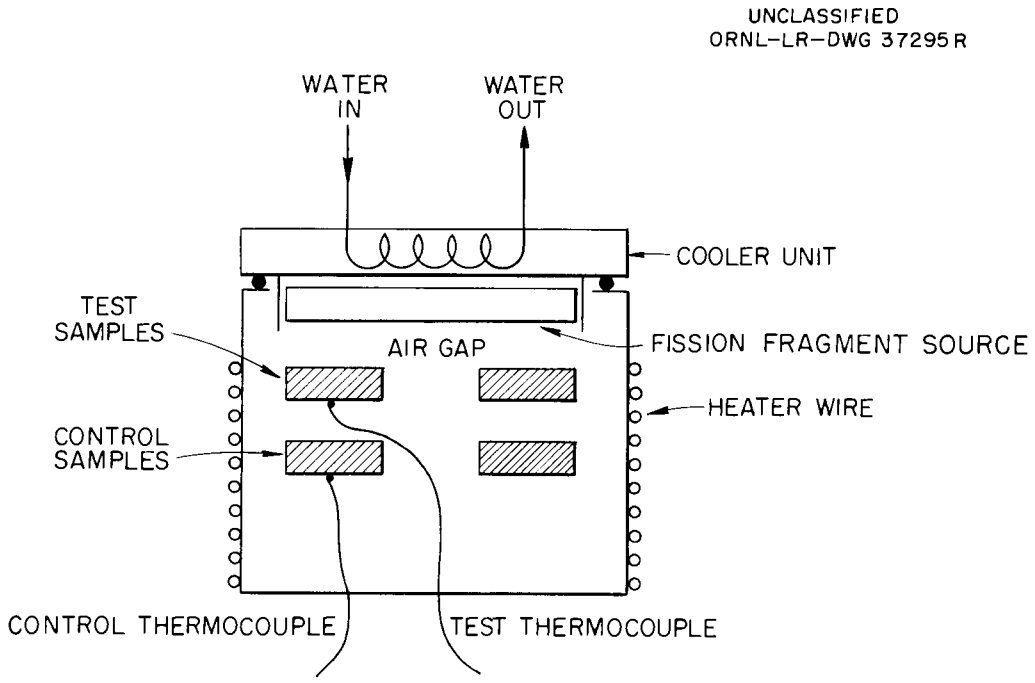

Fig. 1. Schematic Diagram of Assembled Autoclave Unit.

Y-29282

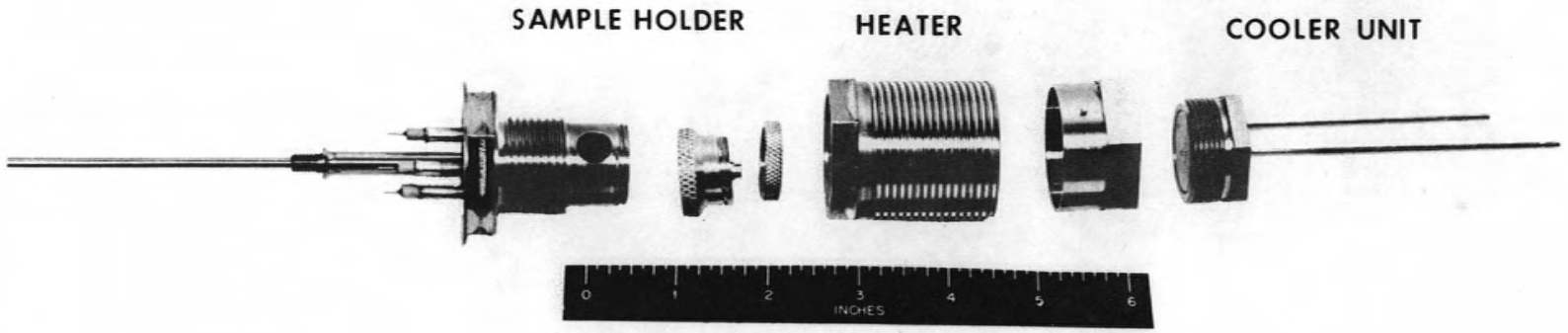

Fig. 2. Components of Autoclave.

Y-29281

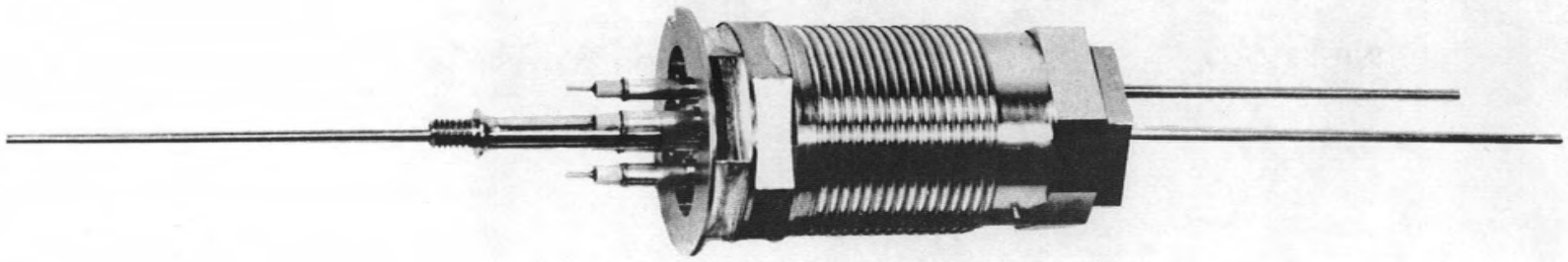

Fig. 3. Assembled Autoclave Unit.

than 90% of the theoretical density. Each disc was 0.80-in. diameter, and the average thickness of the fission fragment recoil source within each disc was 0.0171-in. Total weight of U^{235} per disc averaged 0.359 grams.

Heater Unit

External heat had to be supplied to maintain the zirconium specimens at the desired temperature. This was accomplished by winding insulated nichrome wire around the grooved portion of the aluminum bronze heater body. In order to provide a thermal barrier to retard the rate of heat transfer from the aluminum bronze to the fission fragment recoil source, a hollow cylindrical piece of stainless steel was silver-soldered onto the end of the grooved portion of the heater body. Stainless steel is a relatively poor heat conductor having a thermal conductivity which is 20% of that of aluminum bronze. The fission source-cooling unit was mounted in this section of the assembly.

Zirconium Specimens and Specimen Holder

The specimen holder, fabricated of aluminum bronze, held four zirconium specimens in place. Geometrically, the specimens approximated half discs and all had equal surface areas. A pair were placed approximately one millimeter away from the fission fragment recoil source with one surface of each specimen exposed to recoil bombardment. These samples were designated as the test samples. The remaining two discs, the control

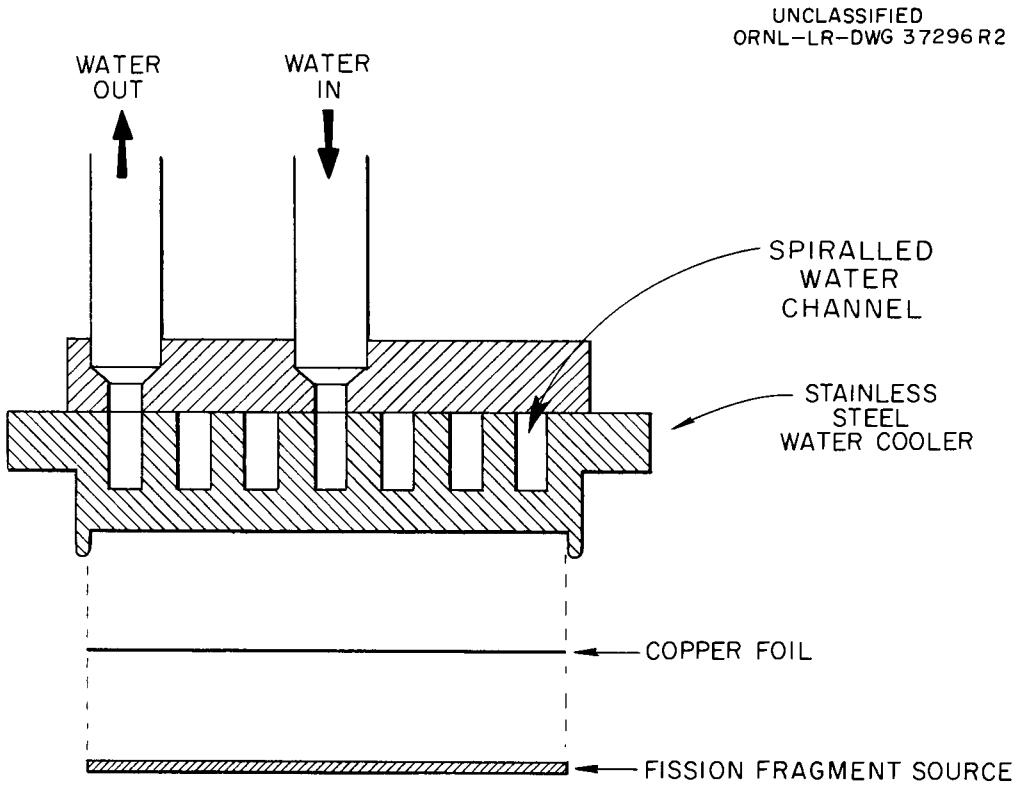

Fig. 4. Schematic Diagram of Cooler Unit.

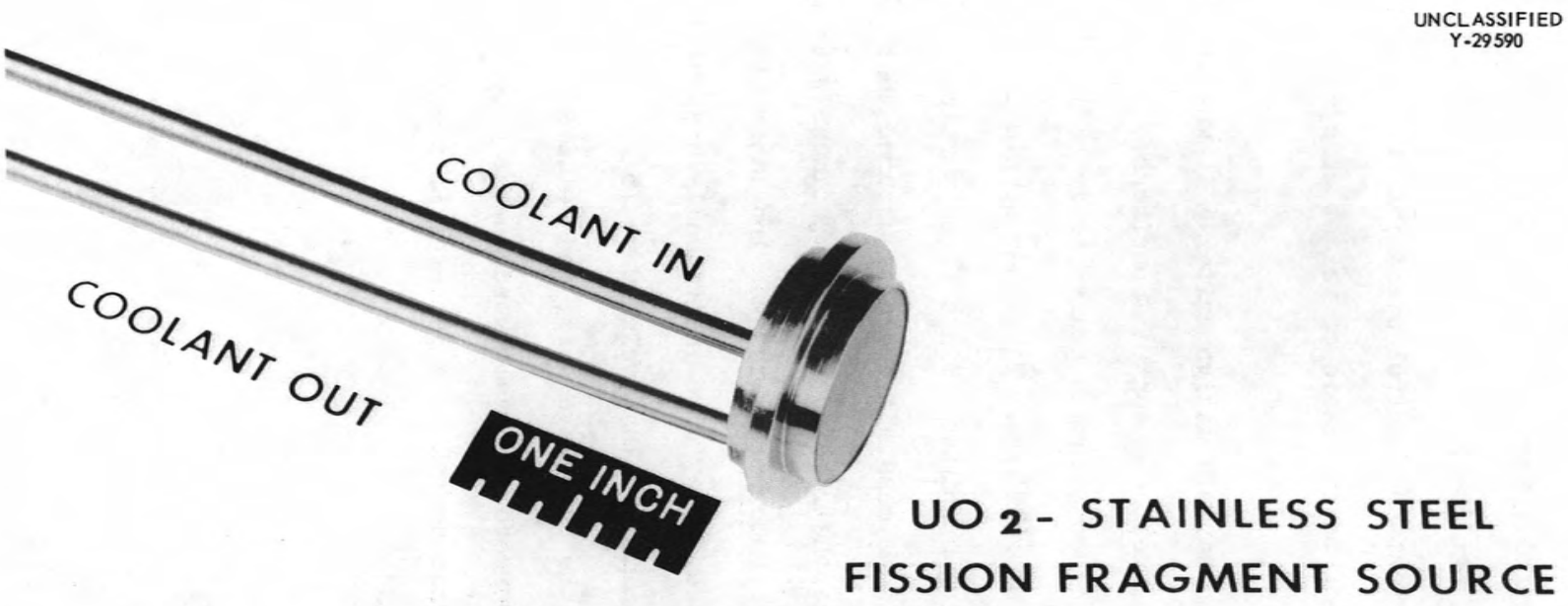

Fig. 5. Assembled Cooler Unit.

samples, were located in back of the test specimens and except for the fission fragment recoils were exposed in approximately the same radiation environment. At the conclusion of the series of experiments, a comparison of the test and control specimens, both irradiated and non-irradiated, was made on the basis of weight change and individual surface characteristics.

In order to satisfy design criteria it was necessary to have a pair of each of the test and control specimens. One of each pair had a thermocouple (iron-constantan) peaned to it to monitor the temperature of each type of specimen. The other specimen of each pair was used as the weighing specimen. Since these particular specimens had approximately the same mass, it could be assumed that they were at the same temperature as their corresponding specimens with thermocouples. Each of the bare thermocouple wires was insulated with ceramic beads within the autoclave. They were individually brought through hermetic seals (ceramic to metal seals), which were integral parts of the sample holder section of the autoclave unit, and soldered to them.

A third thermocouple was peaned to the exterior wall of the heater section. This served as a detector in the temperature control circuit.

Instrumentation

Instrumentation for these experiments was relatively simple. The temperature of both test and control samples were continuously monitored by a twelve point Brown recorder. The thermocouple on the external wall of the heater was attached to a Brown "Electronik" controller. With this instrument temperature variations under steady-state conditions were only $\pm$ 0.5°C.

Cooling of the fission fragment recoil source was accomplished by the use of plant demineralized water. To reach the experiment while inserted in the reactor, water had to travel through 21 feet of 1/4" O.D. 2S aluminum tubing. Hence the plant water was pressurized with a 3/4 horsepower centrifugal pump in order to maintain adequate flow. A portion of this main water stream was diverted to the experiment by means of a valving system.

Instrumentation was provided to give sufficient protection against cooling water flow stoppage. Minneapolis-Honeywell Pressurtrol units were installed at both the inlet and exit water lines at the face of the reactor. In the event of appreciable impairment of flow, relays were set to activate a reactor shutdown until the trouble could be found and remedied. This precautionary measure was taken to prevent overheating.

CHAPTER VI

EXPERIMENTAL PROCEDURE

In order to make one experiment comparable with another it was necessary to standardize the initial conditions of each run. This involved devising a scheme to be able to reproduce two things reliably: the surfaces of each zirconium specimen and the environment in the autoclave in which the specimens were exposed. The procedure which was adopted involved several steps. All of the specimens were chemically polished and then, like the autoclave components, were degassed and preoxidized for a specified time before the actual run. This preoxidation step was necessary for safety reasons: each experimental unit had to be successfully pre-run at the prescribed operating conditions out-of-pile before actual insertion into the reactor.

Preparation of Zirconium Specimens and Autoclave Assembly

The zirconium specimens were made from crystal bar stock furnished in the form of a cold rolled sheet, 0.025-in. thick, by the Metallurgy Division of ORNL. This metal had the following nominal spectrographic analysis: 100 ppm hafnium, 200-500 ppm iron, 200 ppm nickel, and less than 100 ppm each of titanium, aluminum and silicon. Samples in the form of half discs were machined from this sheet. Each specimen weighed approximately 0.4 grams and each side of the disc had a surface area of 1.2 cm^2.

The surfaces of all zirconium specimens were chemically polished in a solution of 50% distilled water, 45% concentrated nitric acid and 5% hydrofloric acid (48%). Each disc was alternately put into polish solution for one or two minutes and then in distilled water until the surfaces appeared visually to be smooth and bright. In order to achieve uniform polishing, the specimen had to be manually agitated even though the polish solution was magnetically stirred. Quick transfer of the disc to vigorously boiling distilled water removed trace quantities of polishing solution. This was followed by successive rinses in ethyl alcohol, ethyl ether and petroleum ether. A jet of oxygen rapidly evaporated the solvent film. Each sample was then weighed on a five-place semi-micro balance which had a reproducibility of $\pm$ 0.01 mg. The same balance was used to obtain all weight gains recorded in this report.

The components of each autoclave were uniformly pretreated before the assembly of an experiment. They were degassed for successive 24 hour intervals at room temperature and at 100°C at $<10^{-3}$ mm Hg. Then the components were oxidized at 290°C for 24 hours in high purity oxygen. The oxygen used throughout this series of experiments came from the same source and had the following analysis: 99.63% O_2, 0.42 $\pm$ 0.10% H_2 + CO and negligible non-combustibles.

At the completion of these preliminary operations, the zirconium specimens were positioned properly within the autoclave and the unit was assembled. The out-of-pile operations performed prior to insertion into

the reactor are outlined below:

1. Unit degassed for successive 24 hour intervals at room temperature and 100°C (test sample temperature) at $<10^{-3}$ mm Hg.
2. Unit oxidized at 250°C (test sample temperature) for 24 hours in high purity oxygen and cooled.
3. Unit charged with high purity oxygen to one atmosphere pressure at room temperature. System isolated and canned for one week experiments. Two week runs provided with a system such that oxygen could be added daily.
4. Unit run at 250°C (test sample temperature) for 24 hours for the purpose of testing the reliability of operation of experiment.

Even though all units were able to maintain a vacuum of $<10^{-3}$ mm Hg for 24 hours at 100°C, this did not guarantee that the units were satisfactorily leak-tight or that leaks would not develop during a run. It is conceivable that during the course of a run oxygen could have leaked out of the system slowly. If the leak was large enough, the experiment would have operated not far from atmospheric pressure. As the zirconium specimens consumed oxygen, the gas pressure would have decreased further. Subsequently, air from the surroundings of the experiment could have leaked into the system. Water vapor and nitrogen in this air could have contaminated to some degree the oxygen environment. This

possibly could have influenced the results slightly.

Conditions of Each Experiment

All irradiation experiments were run in Hole 16 of the ORNL Graphite Reactor where the neutron flux was 8.5×10^{11} neutrons/cm^2 second. In general, each component functioned properly during a run and without incident.

A typical set of operating conditions is tabulated below:

Temperature	
Test Samples	- 250°C
Control Samples	- 265°C
Heater Wall	- 285°C
Fission Fragment Recoil Source	- 65°C
Pressure (at room temperature)	- 15 psia (initially)
Cooling Water	
Flow Rate	- 1200 cc/min (max)
Inlet Pressure	- 65 psi
External Heat Source	
E.M.F.	- 30 volts
Current	- 4.0 amps
Power	- 120 watts
Estimated power generated In fission fragment recoil Source while in a neutron flux	- 8-10 watts

A series of five tests was made. Runs Z-5, Z-6 and Z-7 were each one week exposures in the reactor. The fission fragment recoil source was omitted from the latter experiment in order to isolate any effects on the

specimens due to neutron flux environment alone. Runs Z-8 and Z-9 were both two weeks long; the former inserted into the reactor, the latter run out-of-pile as a control test. Table I gives an account of the nuclear conditions for each experiment performed and a brief discourse on this table is given below.

In order to estimate the damage on the zirconium specimens by heavy nuclear particles it was necessary to calculate the energy and intensity of fission fragments being emitted at the surface of the source and impinging on one surface of the test specimens. This was done by calculating the rate of fissioning in the source and then estimating the fraction of the fission fragments formed which were emitted from the surface of the source.

The rate of fissioning in the source was proportional to the thermal neutron flux present. This flux was related to the average thermal neutron flux in the zirconium specimens. It was possible to determine this specimen flux by an activation analysis of the zirconium samples which were present. A brief outline of this method is given in Appendix B.

Because uranium has a high thermal neutron absorption cross section, the flux was depressed at the source. Therefore a correction factor had to be applied to the flux calculated at the zirconium samples to obtain an adjusted corresponding flux in the source. Extrapolation of the data reported by Klima and Ritchie[15] indicates that a plane indium foil of absorption cross section equivalent to that of the U^{235}

UNCLASSIFIED
ORNL-LR-DWG. 39141

TABLE I

SUMMARY OF NUCLEAR CONDITIONS OF EACH FISSION FRAGMENT RECOIL EXPERIMENT

Run	Conditions	Reactor Energy (3.5 Mwhrs)	Average Thermal Neutron Flux at Zr Samples (neutrons/cm^2-sec)	Approximate Thermal Neutron Flux at Fission Fragment Recoil Source (neutrons/cm^2-sec)	Calculated Fission Fragment Intensity at Zr Sample Surface		Estimated Zr Atomic Displacement Production Rate (Displacements/cm^2-doy)	Estimated Fraction Zr Atoms Displaced Within Range of Fission Fragments		Equivalent Integrated Fast Neutron Flux (2 Mev Energy) To Give Same Fraction of Displacements	
					(Particles/cm^2-sec)	Equivalent Solution Power Density (watts/ml)		(Atoms Zr Displaced/Atom Zr cm^2-Range-Day)	(Total Fraction at End of Run)	(nvt/day)	(Total nvt at end of Run)
Z-5	UO_2 Irradiated 1 week	146	5.7×10^{11}	5.1×10^{11}	7.1×10^{8}	16	2×10^{18}	10×10^{-2}	0.7	3×10^{19}	2×10^{20}
Z-6	UO_2 Irradiated 1 week	147	4.0×10^{11}	3.6×10^{11}	5.0×10^{8}	11	2×10^{18}	7×10^{-2}	0.5	2×10^{19}	1×10^{20}
Z-7	$NoUO_2$ Irradiated 1 week	150	4.9×10^{11}	—	—	—	—	0.001×10^{-2}	0.0001	4×10^{15}	3×10^{16}
Z-8	UO_2 Irradiated 2 weeks	300	4.3×10^{11}	3.9×10^{11}	5.5×10^{8}	12	2×10^{18}	8×10^{-2}	(1.1)	2×10^{19}	3×10^{20}
Z-9	UO_2 Out-of-Pile 2 weeks	—	—	—	—	—	—	—	—	—	—

present in the enriched uranium dioxide-stainless steel source employed, depresses the thermal neutron flux by approximately 24%. However for the geometry of this experiment, it was estimated that the flux depression due to the presence of uranium amounted to about 10%.

Knowing this adjusted flux value it was possible to calculate the fraction of fission fragment recoils impinging on the exposed surface of the test specimens. For the particular composition of uranium dioxide and stainless steel used in the source, the range of fission fragments in this material was estimated to be 7 microns. Thus the net intensity of fission fragments bombarding the surface of the specimens was calculated to be 25% of all the fission fragments formed within 7 microns of the surface of the source. This was estimated to be 6×10^8 particles/cm^2/second as seen in Table I. The derivations and methods employed for this calculation are shown in Appendix C, Section I.

The average fission fragment recoil intensity for the three experimental runs (6×10^8 particles/cm^2/second) containing a source may be compared to an intensity of 4.5×10^8 particles/cm^2/second obtained with a dilute uranyl sulfate solution having a power density of 10 watts/ml. This calculation for the aqueous solution assumed that the solution was essentially water and that the range of fission fragments in water at 250°C is 30 microns.

It was convenient to express the potential extent of heavy nuclear particle damage to the zirconium specimens in terms of the fraction of the total number of zirconium atoms displaced within a volume equal to

the product of the surface area exposed to recoils and a thickness equivalent to the range of fission fragments in zirconium. This range, as seen in Appendix C, Section II, was calculated to be 5.5 microns. The number of atoms displaced within this volume of solid was the product of the production rate of displaced atoms and the time that the specimens were exposed to fission fragment bombardment. To estimate the production rate of displaced atoms, a factor[12] was assumed of 10^5 displacements in zirconium for absorption of a fission fragment of full (80 Mev) energy. It was also assumed that for the spectrum of fission fragment energies involved here, the absorption of 80 Mev of energy produced 10^5 displacements.

The estimated values of the fraction of the atoms displaced within range of fission fragments in zirconium expresses only the magnitude of the number of atoms that would have been dislocated were it not for radiation and thermal annealing which were present.

Finally it was of interest to express the heavy nuclear particle damage within the range of fission fragments in zirconium in terms of an equivalent integrated fast flux whose average neutron energy is 2 Mev. In the Graphite Reactor at ORNL the fast flux of neutrons, greater than 1 Mev energy, is considered to be approximately 10% of the thermal flux.[16] Thus an estimate of the fast flux damage to zirconium could be made for specimens of run Z-7, the experiment exposed to a neutron flux for one week without the recoil source. This calculated damage could then be compared to the potential extent of damage produced by fission fragments

expressed in terms of an equivalent integrated fast neutron flux. It has been estimated,[17] for copper, that 10% of the atoms are displaced after being exposed to a fast flux of 10^{13} neutrons/cm^2/second (2 Mev neutrons) for one month, that is, a total nvt of 10^{19} neutrons/cm^2. This same factor was applied to zirconium for estimation purposes. Since the fraction of the number of zirconium atoms displaced within range of fission fragments had been calculated previously, it was possible to estimate, by a proportionality, the integrated fast flux (2 Mev neutrons) equivalent to the damage done by the heavy nuclear particles within the range of fission fragments in zirconium.

It is seen from the last column of Table I that the zirconium atomic displacements due to fission fragments was 10^4 times greater than that due to the actual fast flux that was present in all of the irradiated experiments. The zirconium specimens in run Z-7 were exposed to an estimated integrated fast flux of 10^{16} neutrons/cm^2. This fast flux displaced only a small fraction of the zirconium atoms in the material within range of fission fragments. Zirconium test specimens in the other in-pile runs were exposed to fission fragment bombardment in addition to the same integrated fast flux. The fraction of zirconium atoms displaced by fission fragments was larger by orders of magnitude than that due to fast neutrons and it can be estimated that, in order to produce the fraction of displacements by fast neutrons, an integrated fast flux of 10^{20} neutrons/cm^2 would have been required.

Consideration was also given to the possibility of uranium evapo-

rating from the source and depositing on the zirconium specimens. For this case, a fission fragment intensity different from the calculated value would have prevailed. It has been reported[18] that, in a vacuum of 10^{-4} mm Hg, 1200 atoms of U^{233} were evaporated from a cleaned surface of the metal per fission fragment emitted. Assuming that the present experiments were performed in a vacuum, the source was of cleaned uranium metal and the average fission fragment intensity was 5×10^{8} fission fragments per cm^2-second, there would have been approximately 4×10^{17} uranium atoms evaporated in one week per cm^2 of surface area and deposited on the zirconium specimens. This would represent about 10% of the calculated total number of uranium atoms present per unit of surface area in the source which are within fission fragment range of the surface. Energywise, the fragments from fissioning of uranium deposited directly on the zirconium specimen surfaces would be, proportionally, about 50% as effective as the fragments emitted from the source and would represent a significant amount of energy deposition in the specimen surfaces.

Two conditions in the actual experiments probably minimized any consequences due to uranium evaporation. Because the source employed was fabricated from UO_2-stainless steel, the rate of evaporation of uranium from the source was probably less than that for a cleaned surface of uranium metal. Those uranium atoms which might have evaporated from this source would have had a good probability of colliding with molecules of the gas environment present in the experiments, and a small probability

of impinging directly on the zirconium specimen surfaces. Results of several x-ray diffraction analyses made on oxide and metal scraped from the surfaces of some of the zirconium specimens gave no indication of any significant traces of uranium present.

Post-Irradiation Procedure

After the desired irradiation period, each assembly was retracted into a concrete shield within the experimental hole of the reactor for one week to allow radioactivity decay time and thus ease the handling problems. The assembly, subsequently, was removed to a lead carrier, transported to a remote handling facility and the experiment disassembled.

The remote disassembly of each experimental unit included the following sequence of operations:

1. Removal of the outer aluminum can.
    a. Clamped experimental unit in a vise.
    b. Cut open the can with a power driven saw.
    c. Pulled the autoclave out of the can with the aid of remote manipulators.
2. Separation of the sample holder section from the rest of the autoclave assembly.
    a. Clamped the heater and cooling unit sections in a vise.
    b. Loosened and unscrewed the sample holder section by remotely putting an open-ended wrench onto the hexed top of the section and applying a torque on the wrench with the aid of the manipulators.
    c. Pulled the section out with the manipulators.
3. Removal of the samples from the sample holder.
    a. Two cardboard boxes were placed in the cell; one to contain the test samples and the other the control samples.
    b. Holding the hexed top of the sample holder section over one of the boxes with one set of manipulators, another set of manipulators was used to twist off the cap which held the test samples in place. The test samples were allowed to drop into the cardboard box. Caution was exercised so that there was minimum contact between the

manipulator fingers and the samples themselves.

c. Similarly the sample holder section was held over the other cardboard box and the cap holding the control samples in place was twisted off, the control samples dropping into the cardboard box.

d. Each box was covered.

4. Removal of the samples from the remote handling cell and storage.

a. The cardboard boxes containing the samples were removed to a compartment of the cell where the radioactivity was small compared to the dismantling facility itself. Here the respective samples were dropped into two other clean cardboard boxes with the aid of manipulators. The manipulator fingers did not touch the samples.

b. The clean boxes containing samples were brought out into the room and put into a clean plastic bag. The plastic bag was sealed with tape and put into a lead safe until the samples were examined.

CHAPTER VII

RESULTS

As mentioned previously, in addition to measurement of weight changes of the zirconium specimens, several methods were utilized to study the surface features of the zirconium specimens. They included visual comparison of the surface interference colors, microscopic examination of the surfaces at both high and low magnification using normal and polarized light, study of replicas of the sample surfaces by electron microscopy, and low angle electron diffraction studies to try to identify the structure of the oxide film on the surface seeing the fission fragment recoils.

Weight Change

A summary of the weight change data obtained appears in Table II. Because of difficulties with remote handling techniques in disassembling the Z-5 and Z-6 experiments, it was not possible to obtain accurate weights of the samples at the conclusion of these tests. All weighings recorded in the table were made on a five-place semi-micro balance which had a reproducibility of $\pm$ 0.01 mg.

There were two distinctions between the various test and control samples: namely, temperature and environment. The test samples were maintained at 250^{o}C and one surface of each sample was subjected to fission fragment recoil bombardment. The control samples ran at a

TABLE II

WEIGHT CHANGE DATA

Conditions	Run Number				
	Z-5 UO_2 One Week Irradiation[b]	Z-6 UO_2 One Week Irradiation[b]	Z-7 No UO_2 One Week Irradiation	Z-8 UO_2 Two Weeks Irradiation	Z-9 UO_2 Two Weeks Out-of-Pile
Test Sample[a] (250°C)	—	—	$^{+}0.05_5$ mg	$^{+}0.10_0$ mg	$^{+}0.02_0$ mg
Control Sample[a] (265°C)	—	—	$^{+}0.03_0$ mg	$^{+}0.10_8$ mg	$^{+}0.03_0$ mg[c] $^{+}0.04_0$ mg[c]

[a]TOTAL SURFACE AREA OF EACH SAMPLE WAS 2.4 cm^2.

[b]SAMPLE WEIGHT DATA OBSCURED WHILE DISASSEMBLING EXPERIMENT IN REMOTE CELL.

[c]WEIGHT DETERMINATION ON TWO CONTROL SAMPLES.

temperature of approximately 265°C and in general, except for the recoils, they saw the same radiation environment. The difference in operating temperature between the test and control samples was caused by the presence of the cool surface of the source immediately adjacent to the test samples.

It is of interest to note that the weight gains obtained in run Z-9, the out-of-pile run, are in the same range as those estimated by extrapolating the results of the work of Gulbransen and Andrew[19] on the gaseous oxidation of zirconium to the 250-265°C temperature range.

Visual Examination of Specimens

A visual examination of the specimens was made to observe any differences in interference colors on the respective surfaces. An attempt was made to approximate a film thickness from the observed interference colors of each surface.

Unfortunately, a relationship between interference colors and film thickness for zirconium heated in oxygen or air has not been reported. However Boyd[20] has studied this relationship for films formed anodically on Zircaloy-2 for film thicknesses ranging from first order interference to greater than 6000 Å. His technique essentially duplicated that employed by Charlesby[21] in his work on zirconium. Boyd, by using the same linear relationship, reported by Polling and Charlesby,[22] of film thickness to voltage, 30 Å per volt, has obtained the data given in Table III. For this series of experiments, Boyd's

data on Zircaloy-2 were employed for film thickness interpretation because interference color data of Flint, Polling and Charlesby[23] on zirconium are reported to approximately 2000 Å only. This was inadequate to interpret the experimental interference color data obtained in this work.

This interference color-thickness relationship was employed to obtain an approximation of the film thickness on the respective surfaces of the specimens. It is emphasized, however, that the information available is such as to permit only rough estimates of film thickness. The color chart of this table was employed on the assumption that any disparities in formation voltage of anodized films between zirconium and Zircaloy-2 are not as large as one order of interference colors or approximately 1000 Å. Also, the table was used with the supposition that there is little difference in the film color-thickness relationship between thermally formed films and those prepared anodically. This should be a reasonable assumption based on the findings of Polling and Charlesby[24] and confirmed by Pemsler[25]; however Misch and Gunzel,[26] among others, dispute its validity. It was also assumed that there were no radiation effects on the optical properties of the oxide film such as on refractive index and dielectric constant.

It is only under these assumptions that Table III was used, both in this section and the next one, to estimate film thickness from the interference colors of the specimen surfaces. Figure 6 shows the scheme

TABLE III

OPTICAL THICKNESS OF ANODIC FILMS ON ZIRCALOY-2

Optical Thickness (30 Å per volt) Å	Film Color
150	Yellow
300	Gold
400	Reddish-Purple
450	Purple
600	Blue
1000	Very Light Blue
1300	Yellow
1650	Orange
1800	Red-Purple
2100	Purple
2400	Blue
2700	Bluish-Green
3000	Green
3300	Gold
3600	Red-Purple
3900	Purple
4200	Blue-Green
4500	Green
4800	Green & Rose (mottled)
5100-5500	Rose
5700	Rose & Green
6300	Green

Source: Boyd, C. M., Unpublished work, ORNL

used to identify the various specimen surfaces. Data pertaining to these surfaces are given in Table IV. Again using the format of Figure 6, Figure 7 gives a comparison of the specimen surfaces exposed in runs Z-7 and Z-8 to an out-of-pile oxidized sample and a typical chemically polished specimen.

The weight gains reported in Table IV were calculated from the estimated film thicknesses. For the particular geometry of the sample (surface area of 2.4 cm^2), every 283 Å film thickness was equivalent to 0.01 mg weight gain. This assumed that the over-all reaction was $Zr + O_2 \longrightarrow ZrO_2$, that all surfaces oxidized uniformly, and that all oxide remained on the surfaces.

Microscopic Examination of Specimens-Normal Illumination

After a detailed examination of all specimen surfaces, a consistent difference was found between the surfaces that faced the fission fragment recoil source and those that were exposed to a neutron flux environment only. The effects of the fission fragment recoils on surface appearance were particularly evident on comparison of the protected edge (due to the shoulder of a bronze ring holding the test specimens in place) and unprotected center of the side of the specimen facing the source. Here it was possible, in examining from the very edge inward, to observe a band of interference colors indicating a change in film characteristics. This feature was not exhibited

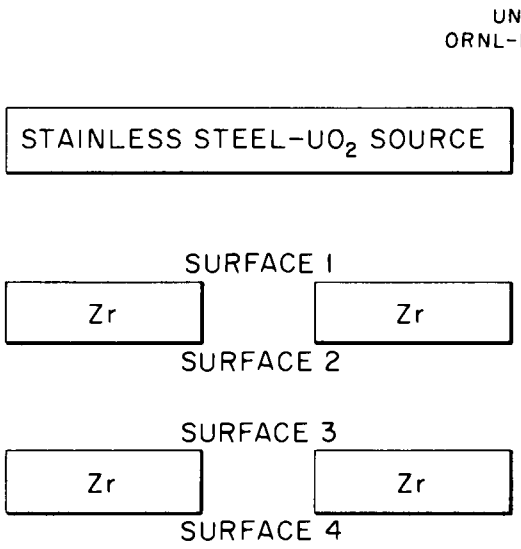

Fig. 6. Configuration of Typical Fission Fragment Recoil Experiment.

TABLE IV

INTERFERENCE COLOR ESTIMATE OF FILM THICKNESS AND WEIGHT GAIN FROM VISUAL SURFACE EXAMINATION

		TEST SAMPLE (250°C)			CONTROL SAMPLE (265°C)		
RUN	CONDITIONS	SURFACE 1	SURFACE 2	ESTIMATED* WEIGHT GAIN (mg)	SURFACE 3	SURFACE 4	ESTIMATED* WEIGHT GAIN (mg)
Z–9	UO_2 2 WEEKS NO RADIATION	DEEP BLUE  500 Å	SAME AS 1	0.02	LIGHT BLUE 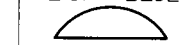 800 Å	SAME AS 3	0.03
Z–8	UO_2 2 WEEKS IRRADIATION	PURPLE AND GREEN, RED AND PURPLE, YELLOW 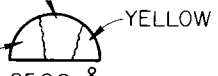 2500 Å	LIGHT BLUE AND YELLOW  1000–1300 Å	0.07–0.08	YELLOW 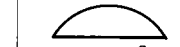 1700 Å	SAME AS 3	0.06
Z–7	NO UO_2 1 WEEK IRRADIATION	LIGHT BLUE AND YELLOW  1000–1300 Å	SAME AS 1	0.04–0.05	YELLOW AND BLUE  1200–1500 Å	SAME AS 3	0.05–0.06

*CONVERSION FACTOR: EVERY 283 Å EQUIVALENT TO 0.01 mg, ASSUMING OXIDATION TO BE UNIFORM ON BOTH SIDES.

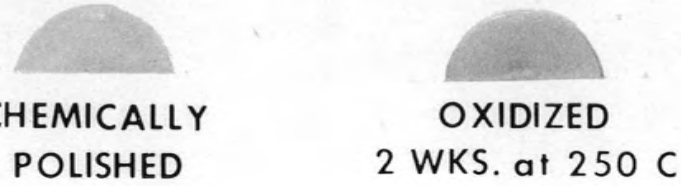

Fig. 7. Effect of Neutron Flux and Fission Fragment Recoils on the Oxidation of Zirconium (Average Thermal Neutron Flux at Samples 4.6×10^{11} neutrons/cm^2/sec at 3.5 Mw).

on the opposite surfaces of the corresponding specimens, the test specimen surfaces in run Z-7, the one week control experiment with no source to furnish recoils, or the corresponding surfaces of the specimens oxidized out-of-pile for two weeks, run Z-9. Figure 8 shows the changes of colors observed at the periphery of a typical surface facing the source. In contrast, Figures 9, 10, and 11, respectively, are representative of the same position on the opposite surface of the same test specimen, the side facing the cooling unit in the absence of a source in run Z-7, and the corresponding surface of run Z-9. A brief description of the interference colors of these figures along with the corresponding film thicknesses as estimated from Table III are given below.

The photograph of Figure 8 corresponded to the left side of surface 1-Z8 on Figure 7. Assuming the blue blotches appearing at the shielded edge of this portion of the surface to be of first order interference, it was possible to follow the various interference colors in order to a mixed gold and red-purple which corresponded to an estimated film thickness of 3500 Å. The right side of this specimen terminated in a green-blue corresponding to a film thickness of 2700 Å.

The back side of this specimen, Figure 9, was predominately a yellow field intermixed with blue and reddish-purple giving a film thickness range of 600-1800 Å. Figure 10, run Z-7, was found to have a light blue field with light yellow blotches corresponding to 1100-1200 Å. There was a blue field with light yellow and purple spots for

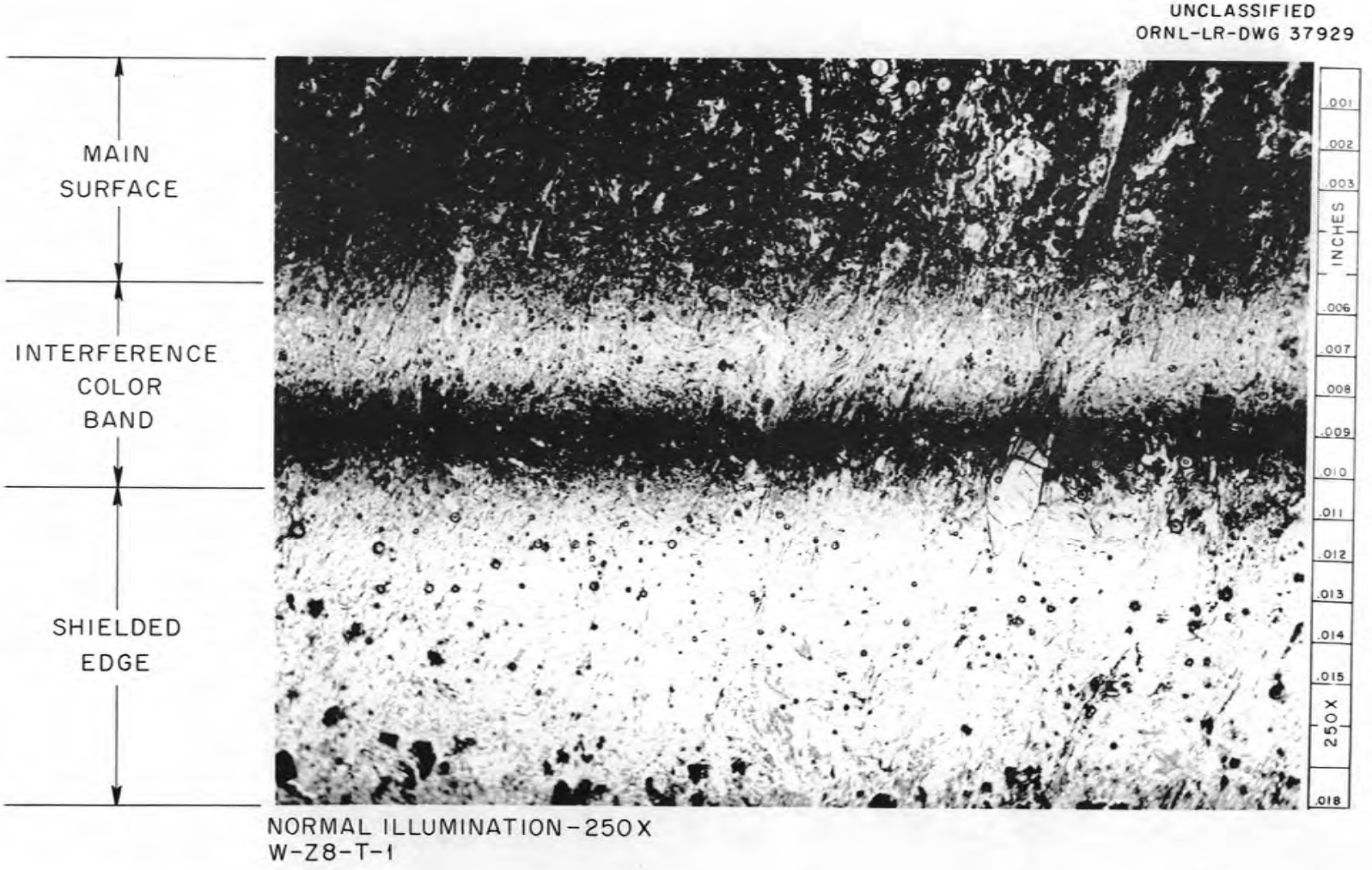

Fig. 8. Periphery of Zirconium Test Specimen Surface Exposed to Fission Fragment Recoils.

UNCLASSIFIED
ORNL-LR-DWG 37928

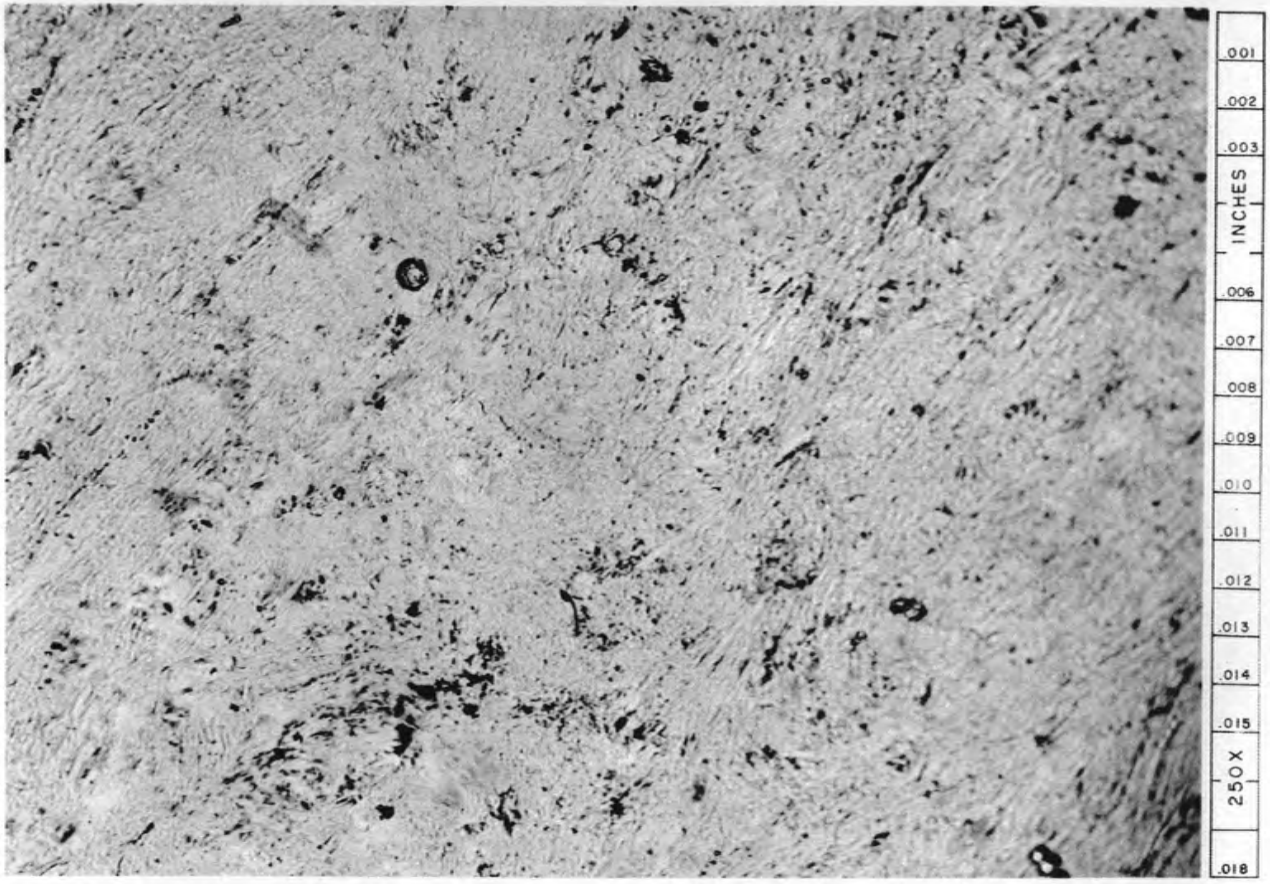

NORMAL ILLUMINATION-250X
W-Z8-T-2

Fig. 9. Periphery of Zirconium Test Specimen Surface Opposite to Side Seeing Fission Fragment Recoils (Exposed in Neutron Flux Only).

UNCLASSIFIED
ORNL-LR-DWG 37927

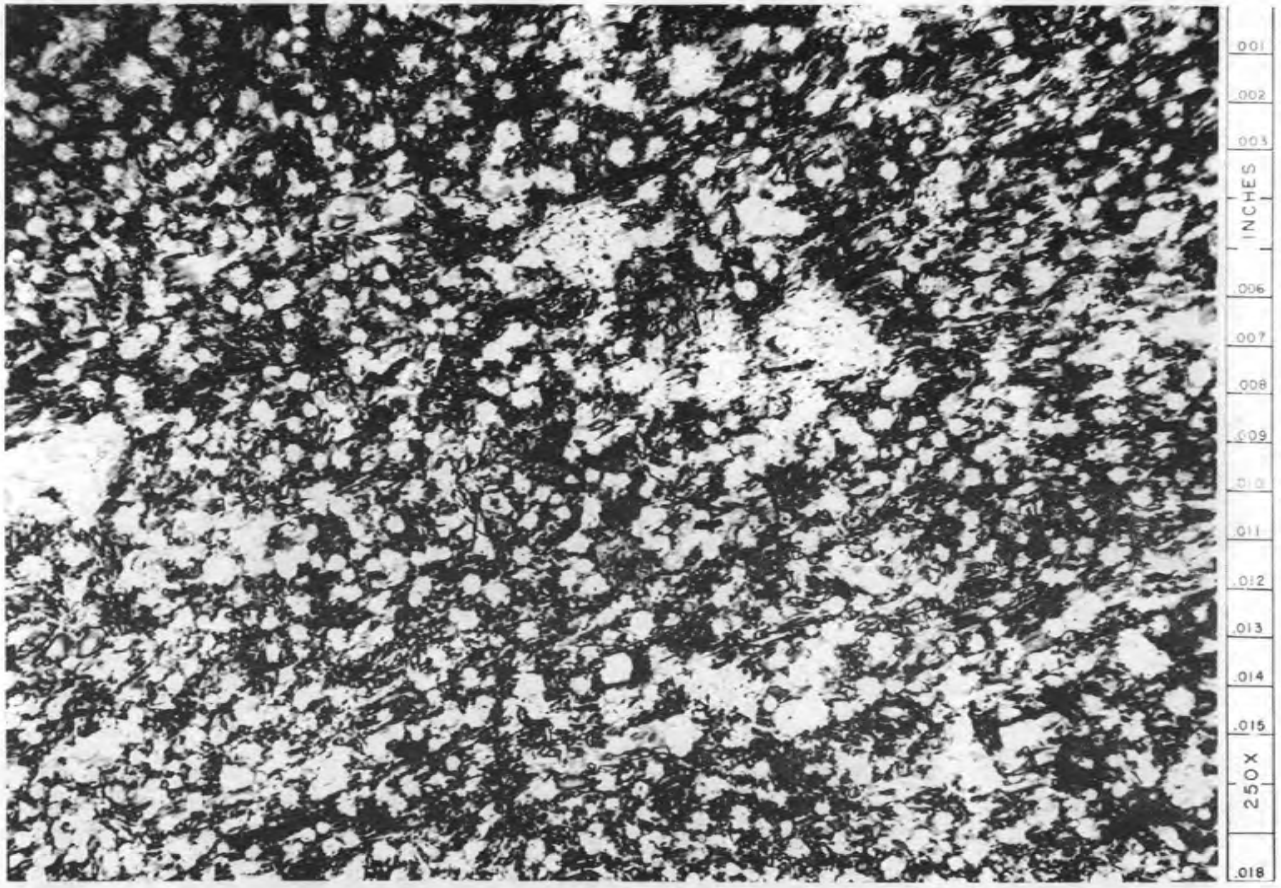

NORMAL ILLUMINATION-250 X
W-Z7-T-1

Fig. 10. Periphery of Zirconium Test Specimen Surface Exposed in Neutron Flux Only.

UNCLASSIFIED
ORNL-LR-DWG 37926

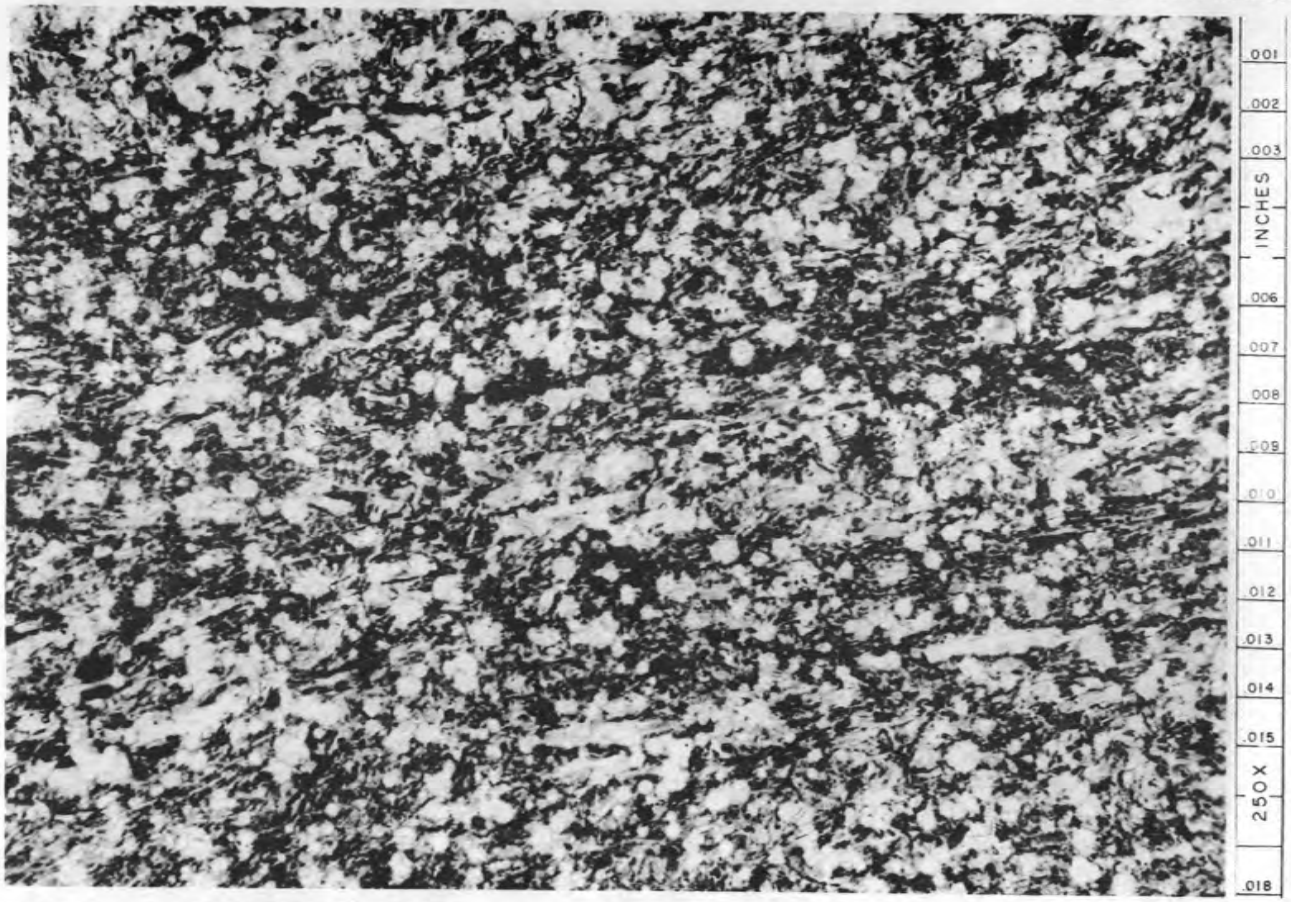

NORMAL ILLUMINATION-250X
W-Z9-T

Fig. 11. Periphery of Zirconium Test Specimen Out of Irradiation Control Run.

run Z-9, Figure 11, for an estimated 600-1000 Å film thickness.

Microscopic Examination of Specimens-Polarized Light

Microscopic examination of the specimens under polarized light showed pronounced differences between the surfaces that were exposed to fission fragment recoils and all other surfaces examined. Only the surfaces seeing recoils were inactive to polarized light. All of the other specimen surfaces, when examined, were responsive to polarized light as the specimen was rotated 180°. Figure 12 shows again the periphery of the same surface exposed to fission fragment recoils as in Figure 8, but this time under polarized light. There is a line of demarcation which divides the surface into two distinct regions: the featureless region corresponds to the surface area that saw fission fragment recoils while the contrasting region is the surface area that was shielded from recoils by the bronze ring holder. Figure 13 is a picture of the opposite surface of the same specimen. The contrasting features in the latter figure are uniformly distributed over the whole surface area.

Electron Microscopy

Palladium shadowed carbon replicas were made of the surfaces of all the specimens used in this series of experiments. Fifteen areas were photographed from runs Z-5, Z-6, and Z-8 on the surfaces seeing

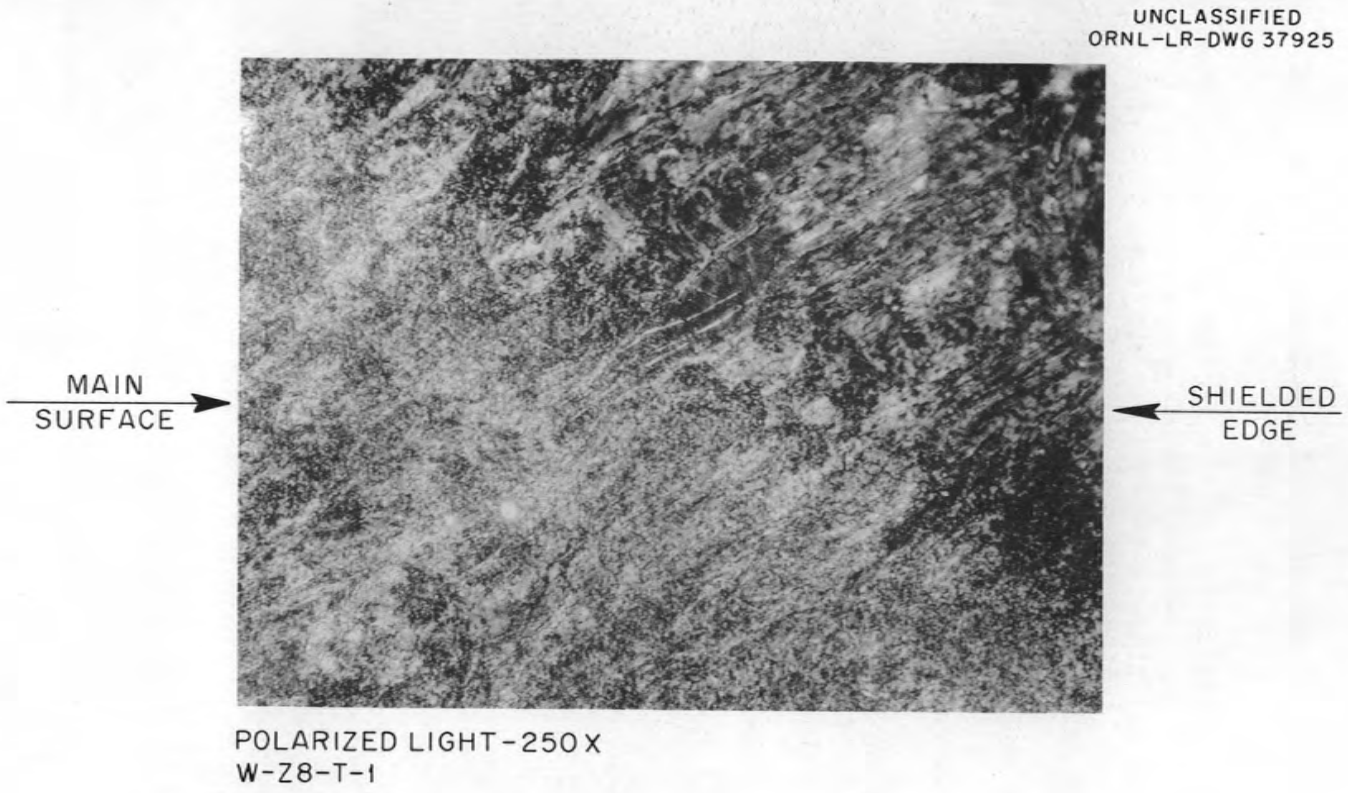

Fig. 12. Periphery of Zirconium Test Specimen Surface Exposed to Fission Fragment Recoils.

UNCLASSIFIED
ORNL-LR-DWG 37924

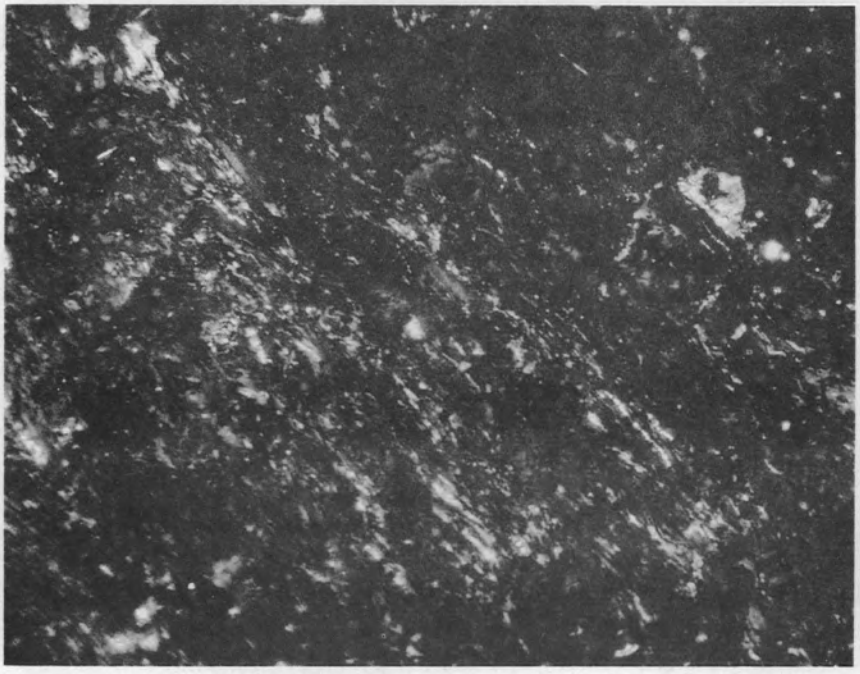

POLARIZED LIGHT-250 X
W-Z8-T-2

Fig. 13. Periphery of Zirconium Test Specimen Surface Opposite to Side Seeing Fission Fragment Recoils (Exposed in Neutron Flux Only).

fission fragment recoils. These electron micrographs in all but two cases indicated a rough mottled surface, an example of which is shown in Figure 14 from run Z-8. The size of the mounds seen in the figure was in the order of 0.5 micron. The surfaces not seeing fission fragment recoils were consistently much smoother as shown for run Z-8 in Figure 15. The size of the pebbles observed was about an order of magnitude smaller than the mounds seen in Figure 14.

Low Angle Electron Diffraction Studies

An attempt was made to identify the structure of the oxide film on opposite sides of a typical test specimen by obtaining low angle electron diffraction patterns for each surface. The pattern of the side exposed to fission fragment recoils appeared to be composed of very diffuse rings. In contrast, the opposite surface showed a pattern of a relatively large number of spotty rings which indicated fewer diffraction centers. The two types of patterns described are shown in Figure 16.

UNCLASSIFIED
ORNL-LR-DWG 37923

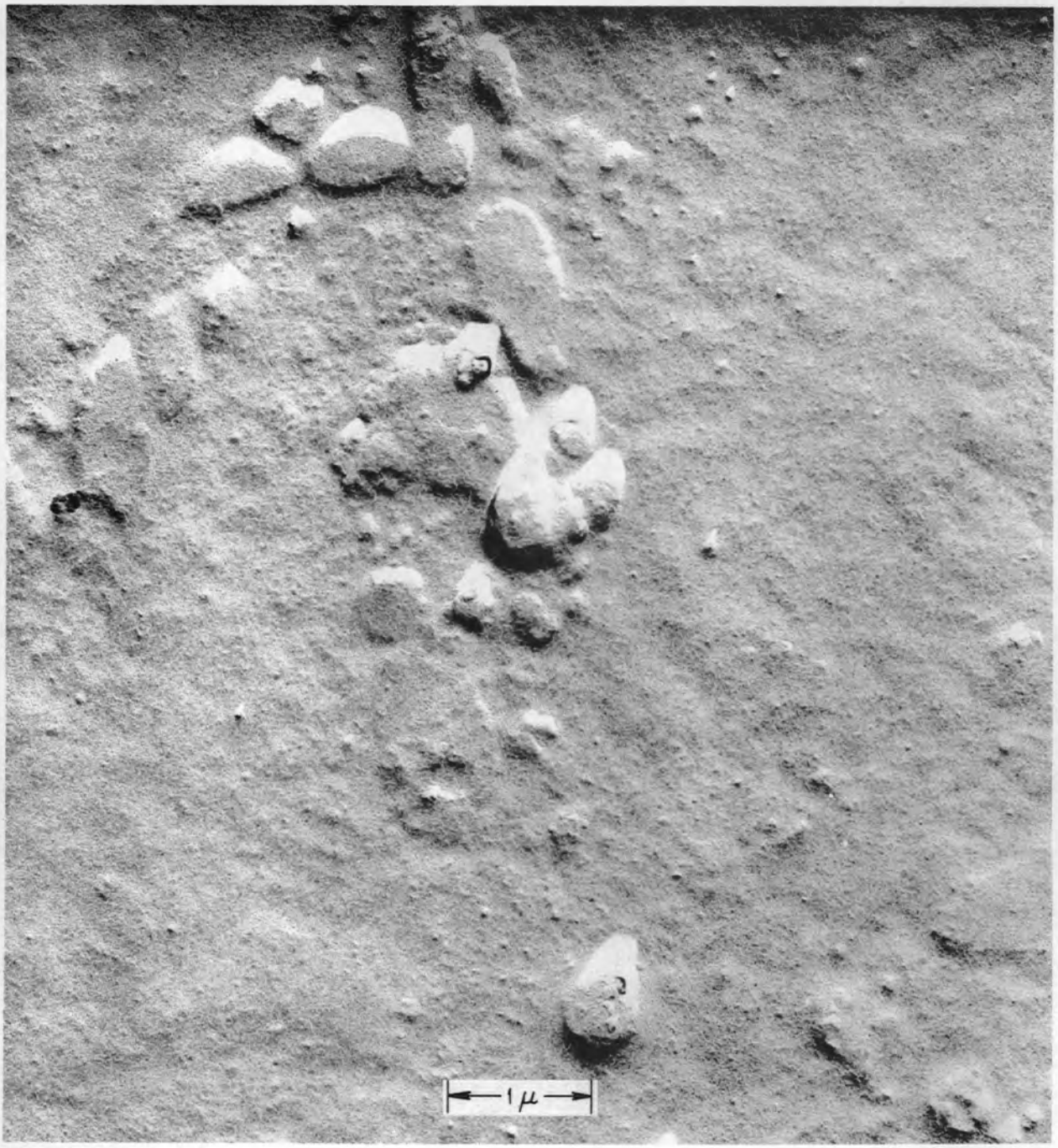

22,700X
W-Z8-T-1

Fig. 14. Surface of Zirconium Test Specimen Exposed to Fission Fragment Recoils (Pd Shadowed Carbon Replica).

UNCLASSIFIED
ORNL-LR-DWG 37922

22,700X
W-Z8-T-2

Fig. 15. Surface of Zirconium Test Specimen Opposite to Side Seeing Fission Fragment Recoils (Exposed in Neutron Flux Only; Pd Shadowed Carbon Replica).

UNCLASSIFIED
ORNL-LR-DWG 37921

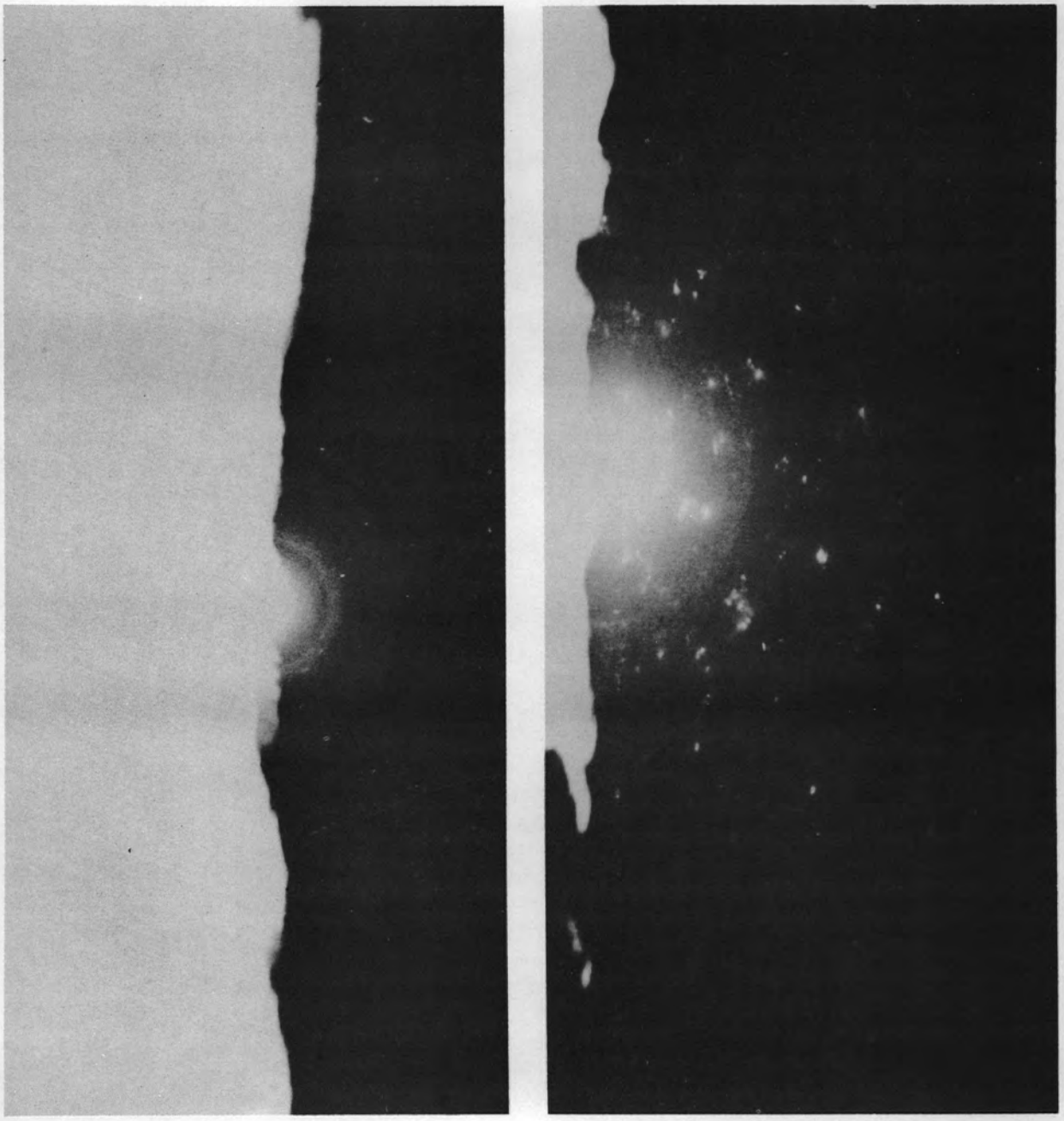

SURFACE FACING FISSION FRAGMENT RECOIL SOURCE.

SURFACE OPPOSITE TO SIDE FACING FISSION FRAGMENT RECOIL SOURCE.

Fig. 16. Low Angle Electron Diffraction Patterns of Surfaces of Test Sample of Run Z-8.

CHAPTER VIII

INTERPRETATION OF RESULTS

Among the different types of analyses made on the specimens of this series of experiments, two of the results are quite positive in nature. They are the patterns obtained by low angle electron diffraction studies and the optical behavior of the surfaces to polarized light. A third less positive result was obtained from the surface topography surveys made on the replicas of the various specimen surfaces. The balance of the analytical methods employed yielded results which were not inconsistent with these findings.

The loss of optical anisotropy as observed by examination under polarized light, with the microscope used, indicated that the oxide film on those surfaces exposed to fission fragment recoils could have undergone a phase change. On the other hand this observed loss of optical anisotropy together with the diffuse ring patterns as obtained by low angle electron diffraction indicated that the normal oxide film on those surfaces exposed to recoils had developed a very fine particle size with random orientation. The evidence indicates that the oxide film on all other surfaces remained highly oriented.

On the basis of the electron microscopy studies of replicas of the various surfaces, there is some evidence-but not really conclusive evidence-that the surface topography was changed as a result of fission fragment recoil bombardment. It should be pointed out once again that

Figures 14 and 15 are only fairly representative of the surface topography of the two types of surfaces. There were a few electron micrographs of the surfaces that were exposed to recoils which did not possess the pustular appearance and appeared to be similar to the surfaces that were exposed to neutron flux only.

Due to the expense of each experiment, it was of value to try to interpret all available data. Although the balance of the methods used for analysis yielded data which were not clearly definable, yet if these data were interpreted with some reasonable assumptions, they would tend to support the findings of the other analyses made.

To interpret the weight gain data obtained, it is necessary to examine Table II once again. In this table, the only comparison that can be reasonably made is between run Z-8 and run Z-9, both two week runs, the former inserted into the reactor and the latter performed out-of-pile. It should be recalled that in both experiments the test specimens were maintained at 250°C while the control specimens, because of the design criteria, assumed a temperature of about 265°C. Therefore this temperature difference is a reasonable explanation for the slightly greater weight gains observed on the control specimens over the test specimens in run Z-9.

There is a greater weight gain in the control specimen of the in-pile run Z-8 than in the corresponding specimens of the out-of-pile run Z-9. This larger weight gain observed for the irradiated control specimen might be attributed to the neutron flux present in run Z-8,

assuming that all other factors are identical.

It is also interesting to note that weight gains for both the test and control specimens are equal in run Z-8. If it is assumed that both test and control specimens were exposed to the same neutron flux environment, then it would be proper to expect that the control specimen would have a slightly greater weight gain than the test specimen because of the higher operating temperature of the former specimen. Yet they are equal. Thus some factor compensated for the lower temperature of the test specimen. The presence of fission fragment recoils on the exposed surface of the test specimen may be one factor that is compensating for its lower temperature.

As added support for this hypothesis, reference is made to Table VI in Appendix B. This table shows the calculated values for the thermal neutron flux in the respective zirconium samples of each run inserted into the reactor. That the flux in the test specimen was consistently lower than that in the control specimen is shown upon a comparison of the values calculated for each of the runs Z-6, Z-7, and Z-8. This adds strength to the supposition that the fission fragment recoils did indeed produce a compensating effect and that it is a reasonable explanation for the equal weight gains observed on the test and control specimen of run Z-8.

Another proposition is suggested by Jenks[27] to explain the weight gain data. The larger weight gain in the control specimen of in-pile run Z-8 as compared to the corresponding specimens in out-of-pile run

Z-9 can be attributed to the activated oxygen environment present in the Z-8 experiment. This activated environment was due to the presence of reactor radiations which might have caused chemical changes in the gas, producing such reactive forms of oxygen as ozone, ions, radicals and excited species. It is well to recall that the fast neutron flux (the energy range of flux which causes atomic displacements) was estimated to be 10% of the thermal neutron flux present. Because the magnitude of the fast flux in the control specimen was small, the presence of activated oxygen might be a reasonable explanation for the larger weight gain observed in the irradiated control sample.

The equal weight gains observed for the test and control specimens of run Z-8 may be explained by an even greater activated oxygen environment in the vicinity of the test specimen due to the presence of fission fragment recoils. Jenks[27] has estimated that the concentration of reactive species of oxygen was 10^3 times greater at the surface of the test specimen exposed to recoils than at the control specimen. Thus the temperature compensating effect which makes the weight gain of the test specimen equal to that of the control specimen may actually be due to the greatly increased activity of the oxygen at the surface of the test specimen exposed to recoils - rather than the fission fragment recoils in the oxide and metal.

The results of the correlation of the interference colors with film thickness tend to support the weight data. Table V compares the measured weight gains with estimated weight gains based on visual and microscopic examination of surface oxide interference colors on specimens of runs Z-8 and Z-9. The film thicknesses of each surface of each specimen as estimated by the use of the color chart, Table IV, is also listed.

It is of interest to note that for the test specimen of run Z-8, the estimated film thickness of surface 1, the surface that was exposed to recoils, is about twice that of surface 2, the surface that was in a neutron flux only. The film thickness evaluated for surface 2, in turn, is less than that for the surfaces of the control sample. This is additional evidence that fission fragments did indeed more than compensate for the lower test specimen temperature of 250°C. Operating at 265°C, the control specimen, in approximately the same neutron flux environment as surface 2 of the test specimen, would be expected to have a greater film thickness than surface 2.

It must be emphasized once again that all of these oxide film thickness estimates are based on four assumptions: (1) the blue color observed at the shielded edge of the surface exposed to fission fragment bombardment was of first order and the other interference colors on the main surface were no greater than third order, (2) the interference colors on the opposite side of the test specimen and both surfaces of

TABLE V

SUMMARY OF ACTUAL AND ESTIMATED WEIGHT GAIN DATA AND ESTIMATED OXIDE FILM THICKNESS – RUNS Z-8 AND Z-9

Run	Specimen		Actual Weight Gain (mg)	Visual Surface Examination		Microscopic Surface Examination	
				Estimate of Film Thickness (Å)	Equivalent Weight Gain (mg)	Estimate of Film Thickness (Å)	Equivalent Weight Gain (mg)
Z-8	Test		0.10_0		0.07–0.08		0.09
		Surface 1		2500		3000	
		Surface 2		1000–1300		1500–1600	
	Control		0.10_8		0.06		0.07–0.08
		Surface 3		1700		2100–2200	
		Surface 4		1700		2100–2200	
Z-9	Test		0.02_0		0.02		0.02–0.03
		Surface 1		500		700–800	
		Surface 2		500		700–800	
	Control (1)		0.03_0		0.03		0.04
	Control (2)		0.04_0				
		Surface 3		800		1100	
		Surface 4		800		1100	

the control specimen of run Z-8 were no greater than second order, (3) the interference colors on the specimen surfaces of the out-of-pile experiment, run Z-9, were in the first order range, and (4) no change in the optical properties of the oxide film due to radiation effects.

CHAPTER IX

CONCLUSIONS AND RECOMMENDATIONS

From the experimental results of these investigations the following conclusions can be stated:

1. The oxide film of the surfaces that saw fission fragment recoils lost its optical anisotropy as shown by examination under polarized light with the microscope employed (750x). This indicates a possibility that these oxide films either underwent a phase transformation or developed randomly oriented grains of a size too small to be resolved with an optical microscope. All other oxide surfaces remained highly oriented and showed resolvable areas of optically active oxide.
2. The low angle electron diffraction study revealed that the surface subjected to recoil bombardment had a structure which produced a diffuse ring pattern while the opposite surface, exposed to a neutron flux only, produced a pattern of a relatively large number of spotty rings. It is consistent with the results of the polarized light studies to conclude that the normal oxide film on the surface that was exposed to recoils possibly had developed a very fine particle size with random orientation.
3. The electron micrographs gave evidence of a difference in the surface that had been subjected to recoil bombardment. Most

of the photogtaphs of these surfaces showed mounds on the surface in the order of 0.5 micron in size. In comparison, most of the other surfaces that were either in a neutron flux or were oxidized out of radiation revealed a pebbly surface with the size of each pebble being about an order of magnitude smaller than the mounds.

4. The limited amount of weight gain data was found to be not inconsistent with the other results.
5. The interference color studies gave qualitative indications of a change in the oxide film thickness of the surfaces exposed to recoils.
6. The data obtained do not provide sufficient information to establish the mechanism of the effects of fission fragment recoils on the oxidation of zirconium.
7. The experimental technique that has been developed is one which can be effectively used to study the fission fragment recoil effects on other metals or alloys.

For any further studies on zirconium, the following recommendations are suggested:

1. The analyses of future results would be greatly aided by using annealed specimens or better yet, large single crystals of zirconium if such could be made.
2. Specimen exposures at higher temperatures, in the order of 300°C, would probably give better quantitative data, particularly with regard to weight change.

LIST OF REFERENCES

1. Jenks, G. H., in Fluid Fuel Reactors (Lane, J. A., MacPherson, H. G. and Maslan, F., Editors), pp. 232-245 Reading, Mass., Addison-Wesley Publishing Co., Inc., (1958)

2. Dewhurst, H. A., Samuel, A. H., and Magee, J. L., "A Theoretical Survey of the Radiation Chemistry of Water and Aqueous Solutions," Radiation Research I, 62 (February, 1954)

3. Jenks, G. H., in Fluid Fuel Reactors (Lane, J. A., MacPherson, H. G. and Maslan, F., Editors), p 242 Reading, Mass., Addison-Wesley Publishing Co., Inc., (1958)

4. Jenks, G. H., in Homogeneous Reactor Project Quar. Prog. Rep., ORNL-2743, (April 30, 1959)

5. Wittels, M. C. and Sherrill, F. A., "Irradiation Induced Phase Transformation in Zirconia," J. Appl. Phy. 27, 643 (June 1956)

6. Wittels, M. C. and Sherrill, F. A., "Fission Fragment Damage in Zirconia," Phys. Rev. Letters 3, 176 (August, 1959)

7. Gulbransen, E. A., in Metallurgy of Zirconium (Lustman, B. and Kerze, F., Jr., Editors) National Nuclear Energy Series Division VII 4, First edition p. 562 New York, McGraw-Hill Book Co., Inc., (1955)

8. Thomas, D. E., in Metallurgy of Zirconium (Lustman, B. and Kerze, F., Jr., Editors) National Nuclear Energy Series Division VII 4, First edition p. 635 New York, McGraw-Hill Book Co., Inc., (1955)

9. Hickman, J. W. and Gulbransen, E. A., "Oxide Films Formed on Titanium, Zirconium, and Their Alloys with Nickel, Copper, and Cobalt," Anal. Chem. 20, 158 (February, 1948)

10. Korobkov, I. I. et al., "Electron Diffraction and Kinetic Investigations of the Reactions of Oxidation of Zirconium and Some of Its Alloys," Proceedings of the Second United Nations International Conference on the Peaceful Uses of Atomic Energy - Properties of Reactor Materials 5, 60 (1958)

11. Schwartz, C. M., Vaughan, D. A. and Cocks, G. G., "Identification and Growth of Oxide Films on Zirconium in High Temperature Water," BMI-793 (December 17, 1952)

12. Brooks, H., "Nuclear Radiation Effects in Solids," Ann. Rev. Nuclear Sci. 6, 215 (1956)

13. Jenks, G. H., in Homogeneous Reactor Project Quar. Prog. Rep., ORNL-2432, 122 (October 31, 1957)

14. Bourgett, D. T. and Beaver, R. J., "Fabrication Procedure of a Chemically and Mechanically Stable Fission Fragment Recoil Source for Application in an Oxygen Atmosphere at 250°C," ORNL-CF-58-12-131 (December, 1958)

15. Klema, E. D. and Ritchie, R. H., "Thermal Neutron Flux Measurements in Graphite Using Gold and Indium Foils," Phys. Rev. 87, 167 (July, 1952)

16. Sisman, O., Private communication (May, 1959)

17. Kinchin, G. H. and Pease, R. S., "The Displacement of Atoms in Solids by Radiation," Repts. Prog. in Phys. 18, 1 (1955)

18. Laptev, F. S. and Ershler, B. V., "Vaporization of Metals by Fission Fragments," The Soviet Journal of Atomic Energy English Translation (Consultants Bureau, Inc., New York) 513 (Number 4, 1956)

19. Gulbransen, E. A. and Andrew, K. F., "Kinetics of the Reaction of Zirconium with O_2, N_2 and H_2," Trans. Am. Inst. Mining Met. Engrs. 185, 515 (August, 1959)

20. Boyd, C. M., Unpublished work, Oak Ridge National Laboratory, Oak Ridge, Tennessee

21. Charlesby, A., "Ionic Currents in Thin Films of Zirconium Oxide," Acta Met. I, 340 (May, 1953)

22. Polling, J. J. and Charlesby, A., "Analysis of the Formation Current in Electrolytic Oxidation of Zirconium," Proc. Phys. Soc. (London) 67B, 201 (March, 1954)

23. Flint, O., Polling, J. J. and Charlesby, A., "The Anodic Oxidation of Uranium," Acta Met. 2, 696 (September, 1954)

24. Polling, J. J. and Charlesby, A., "The Influence of Anodic Oxide Films on the Thermal Oxidation of Zirconium," Acta Met. 2, 667 (September, 1954)

25. Pemsler, J. P., "Diffusion of Oxygen in Zirconium and its Relation to Oxidation and Corrosion," J. Electrochem. Soc. 105, 315 (June, 1958)

26. Misch, R. D. and Gunzel, F. H., "The Electrical Resistance of Oxide Films on Zirconium in Relation to Corrosion," J. Electrochem. Soc. 106, 15 (January, 1959)

27. Jenks, G. H., Private communication (May, 1959)

28. Segre, E and Wiegand, C., "Stopping Power of Various Substances for Fission Fragments," Phys. Rev. 70, 808 (December, 1946)

29. Draley, J. E., Greenburg, S. and Ruther, W. E., "The High Temperature Aqueous Corrosion of Uranium Alloys Containing Minor Amounts of Niobium and Zirconium," ANL-5530 (April, 1957)

30. Baker, J. E., "Calculation Methods for Determination of Neutron Flux and Power Density at In-Pile Loop Specimen Locations from Specimen Activity Measurements and Determination of Average Power Density from Cs^{137} in Loop Solution," ORNL-CF-56-8-178 (August, 1956)

31. Holmes, D. K., Private communication (April, 1959)

32. Fulmer, C. B., "Fission Fragment Studies By Magnetic Analysis," ORNL-2320 (August 5, 1957)

33. Schmitt, H. W., Private communication (April, 1959)

APPENDIX A

ALTERNATE TECHNIQUES CONSIDERED FOR MAKING FISSION FRAGMENT RECOIL SOURCES

APPENDIX A

Initial considerations of a fission fragment recoil source indicated it was desirable to obtain uranium in some concentrated form which would be stable in an oxygen atmosphere at 250-300°C. Several approaches to fabricating such a recoil source were attempted but none were developed successfully. Each had their individual limitations but all had one common failing; no relatively simple and reproducible method for a metallic bond to a cooling unit could be devised.

I. Uranium

Methods of applying a very thin poreless film of gold directly to enriched uranium were considered as a means of retarding the oxidation rate of the metal. Considering the range of fission fragment recoils in gold as about 0.23 mil,[28] the protective envelope would have to be appreciably thinner in order to achieve an adequate recoil intensity. Pin-hole free gold foil 0.1 mil thick was not practically obtainable. Evaporating or sputtering techniques were not feasible either because adherence of such a film depends first on securing an oxide-free uranium surface. This is obtained only with difficulty.

II. Compounds of Uranium

Compacts of a variety of powdered uranium compounds were furnished

by the Ceramics Group of ORNL. Foils of UF_4, UO_2, $UO_3 \cdot H_2O$ and U_3O_8 were made by cold mechanical compression at pressures in the order of 60,000 psi. With such techniques densities of 60-75% of theoretical were attainable. These foils were inserted into an air atmosphere at 200°C and weight changes were recorded at 48, 120, and 141 hours. The UO_2 and U_3O_8 discs indicated the least weight change and therefore the most stable of the powder compacts studied. However all of the thin foils were objectionably friable at the conclusion of the test.

III. Uranium Alloys

Much time was devoted to experimenting with a ternary uranium alloy containing $5\frac{1}{2}$% zirconium and $1\frac{1}{2}$% niobium. Reasonable stability made this alloy a good prospect. In distilled water at 265°C this alloy reportedly corroded at a relatively low rate of 22 mils per year over a test period of approximately one year.[29] Cursory tests in air and oxygen over a 24 hour period at 175°C indicated corrosion rates of 0.78 mil per year and 0.74 mil per year respectively.

However, difficulties encountered in achieving suitable attachment to the cooler finally led to consideration of other materials. Several techniques were employed to try to achieve a good bond for heat dissipation between the ternary uranium alloy and a machinable metal which could be fabricated into a cooling unit. One method tried was simply to mechanically spin a thin disc of the alloy into a fabricated cooling unit. Another bonding attempt was made by canning the alloy in

aluminum bronze and hot-rolling the billet down to the desired thickness of uranium alloy. None of these methods were altogether satisfactory.

APPENDIX B

DETERMINATION OF ACTUAL NEUTRON FLUX IN ZIRCONIUM SAMPLES BY ACTIVATION ANALYSIS

APPENDIX B

It is possible to determine the neutron flux to which the zirconium samples have been exposed while inserted in the Graphite Reactor by comparing the activity of these samples to the activity of a standard zirconium specimen irradiated for a known time in a known flux. In such tests surface cleanliness is essential in that all activity caused by extraneous impurities on the surface must be removed. Therefore each irradiated specimen was severely etched in an $HF\text{-}HNO_3$ solution to completely strip off the oxide film. This left a specimen whose activity was due only to neutron irradiation of the zirconium metal.

When zirconium is exposed to a neutron flux, the isotope Zr^{94} is activated and forms Zr^{95} which is unstable. By a series of negative beta emissions it forms the stable isotope Mo^{95}. The complete scheme is as follows:

$$Zr^{94} \xrightarrow{{}_0n^1} Zr^{95} \xrightarrow[t_{\frac{1}{2}} = 65 \text{ days}]{{}_{-1}\beta^0} Nb^{95} \xrightarrow[t_{\frac{1}{2}} = 35 \text{ days}]{{}_{-1}\beta^0} Mo^{95} \text{ (stable)}$$

$$\lambda_1 = 1.23 \times 10^{-7} \text{ sec}^{-1} \qquad \lambda_2 = 2.29 \times 10^{-7} \text{ sec}^{-1}$$

The activity of a zirconium specimen at any time is then the sum of the radioactive isotopes present, Zr^{95} and Nb^{95}. Since the half-lives of the two isotopes are different it is necessary to express, kinetically, the activity contributed by each one for two cases: namely, the total activity for irradiation time, T, and for decay time, t, before activation analysis.

Below is outlined the procedure employed to calculate the actual neutron flux to which the zirconium specimens were exposed. Table VI follows and gives an accounting of how the neutron flux for each run was computed.

During irradiation time, T, the change in the number of atoms of Zr^{95}, $\frac{dN_1^1}{dT}$, is equal to the difference in the formation of Zr^{95} and the decay of Zr^{95} to Nb^{95} and is represented by the differential equation

$$\frac{dN_1^1}{dT} = V\Sigma_a\phi - \lambda_1 N_1^1 \qquad (B.1)$$

The solution to equation (B.1) is

$$N_1^1 = \frac{V\Sigma_a\phi}{\lambda_1}\left(1-e^{-\lambda_1 T}\right) \qquad (B.2)$$

Similarly, the change in the number of atoms of Nb^{95}, $\frac{dN_2^1}{dT}$, with respect to irradiation time, T, is the difference between the formation rate of Nb^{95} and the decay rate of Nb^{95} to Mo^{95}. In this case, the formation rate of Nb^{95} is exactly the same as the decay rate of Zr^{95}. This equation is

$$\frac{dN_2^1}{dT} = \lambda_1 N_1^1 - \lambda_2 N_2^1 \qquad (B.3)$$

Solving for N_2^1, equation (B.3) becomes

$$N_2^1 = \frac{V\Sigma_a\phi\ (\lambda_2 - \lambda_1) + V\Sigma_a\phi\ (\lambda_1 e^{-\lambda_2 T} - \lambda_2 e^{-\lambda_1 T})}{\lambda_2\ (\lambda_2 - \lambda_1)} \qquad (B.4)$$

The decay time, t, is defined as the period between the termination of irradiation and the start of the activation analysis. During this interval the change in the number of atoms of Zr^{95}, $\frac{dN_1^2}{dt}$,

is simply the rate of decay of Zr^{95}, since this isotope is not being produced. Therefore the differential expression is

$$\frac{dN_1^2}{dt} = - \lambda_1 N_1^2 \qquad (B.5)$$

The integral of equation (B.5) is

$$N_1^2 = N_1^1 e^{-\lambda_1 t} \qquad (B.6)$$

For Nb^{95}, during decay time, t, the change in the number of atoms, $\frac{dN_2^2}{dt}$, may be expressed in the same way as in equation (B.3) but with different superscripts to conform to nomenclature. This equation is

$$\frac{dN_2^2}{dt} = \lambda_1 N_1^2 - \lambda_2 N_2^2 \qquad (B.7)$$

The solution to equation (B.7) is

$$N_2^2 = N_1^1 \left(\frac{\lambda_1}{\lambda_2 - \lambda_1} \right) (e^{-\lambda_1 t} - e^{-\lambda_2 t}) + N_2^1 e^{-\lambda_2 t} \qquad (B.8)$$

All of these equations assume that there is no Zr^{95} in a given sample prior to exposing it to a neutron flux.

At the time of activation analysis, the activity, $\frac{dN^2}{dt}$, of a particular sample is the summation of equations (B.5) and (B.7); i.e., the contribution of the remaining Zr^{95} as well as that of the Nb^{95} present. This may be expressed as

$$\frac{dN^2}{dt} = \frac{dN_1^2}{dt} + \frac{dN_2^2}{dt} \qquad (B.9)$$

Baker[30] has reported a method of determining the neutron flux in an "unknown" by comparing it to a standard. For each sample, $\frac{dN^2}{dt}$

is a function of neutron flux, ϕ, irradiation time, T, decay time, t, and mass. When the standard is compared to an "unknown", the usual procedure is to arbitrarily assign the value of unity to the activity of the standard and normalize the activity of the unknown to that of the standard. This, in effect, expresses both activities in terms of unit mass. Thus it is possible to write a proportionality involving only two variables, neutron flux and time. This is

$$\left.\frac{\phi \frac{dN^2}{dt}}{\text{Relative Activity}}\right|_{\text{Standard}} = \left.\frac{\phi \frac{dN^2}{dt}}{\text{Relative Activity}}\right|_{\text{Unknown}}$$

Since the irradiation and decay times are known for both the standard and the unknown it is possible to solve for $\frac{dN^2}{dt}$ in both cases by using equations (B.2), (B.4), (B.6), and (B.8). The neutron flux to which the standard was exposed is known, so that, by rearranging the above equation, the unknown neutron flux can be calculated. This equation is

$$\phi_{\text{Unknown}} = \phi_{\text{Standard}} \left(\frac{\left.\frac{dN^2}{dt}\right|_{\text{Standard}}}{\left.\frac{dN^2}{dt}\right|_{\text{Unknown}}} \right) \left(\frac{\left.\text{Relative Activity}\right|_{\text{Unknown}}}{\left.\text{Relative Activity}\right|_{\text{Standard}}} \right) \quad \text{(B.10)}$$

TABLE VI

SUMMARY OF DATA NEEDED TO CALCULATE AVERAGE THERMAL NEUTRON FLUX AT ZIRCONIUM SAMPLES FOR EACH RUN

Run	Irradiation Time, T (seconds)	Decay Time, t (seconds)	Zr^{95} Activity, dN_1^2/dt (disintegrations/sec)	Nb^{95} Activity, dN_2^2/dt (disintegrations/sec)	Total Activity, dN^2/dt (disintegrations/sec)	Reported Normalized Activity		Thermal Neutron Flux (neutrons/cm^2/sec)		Average Thermal Neutron Flux at Zr Samples (neutrons/cm^2/sec)
						Test Sample	Control Sample	Test Sample	Control Sample	
Standard	1.1×10^6	11×10^6	35×10^{-3}	16×10^{-3}	51×10^{-3}	1.00	1.00	6.5×10^{11}	6.5×10^{11}	6.5×10^{11}
Z-5	0.54×10^6	15×10^6	10×10^{-3}	6.7×10^{-3}	17×10^{-3}	0.284		5.7×10^{11}		5.7×10^{11}
Z-6	0.56×10^6	13×10^6	13×10^{-3}	8.3×10^{-3}	21×10^{-3}	0.259	0.273	3.9×10^{11}	4.1×10^{11}	4.0×10^{11}
Z-7	0.54×10^6	12×10^6	15×10^{-3}	8.2×10^{-3}	23×10^{-3}	0.340	0.355	4.8×10^{11}	5.0×10^{11}	4.9×10^{11}
Z-8	1.1×10^6	10×10^6	36×10^{-3}	15×10^{-3}	51×10^{-3}	0.650	0.693	4.1×10^{11}	4.4×10^{11}	4.3×10^{11}

APPENDIX C

CALCULATIONS OF VARIOUS PROPERTIES ASSOCIATED WITH THE FISSION FRAGMENT RECOIL SOURCE

APPENDIX C

Assuming that the neutron flux at the fission fragment source is 90% of that at the zirconium samples, it is possible to estimate the intensity of fission fragments impinging on the zirconium sample surface and the average range of fission fragments in zirconium.

I. Estimation of Fission Fragment Intensity on the Surface of Zirconium Specimens

Holmes[31] has estimated the fission fragment intensity impinging on the surface of the test zirconium specimens by making the following assumptions of the fission fragment recoil source: (1) a homogeneous binary mixture of stainless steel and uranium dioxide in the source, (2) uniform neutron flux distribution throughout the thickness of the source, (3) two fission fragments produced per fission event, (4) isotropic scattering of fragments from a point source and (5) edge effects neglected. It is further supposed that the air gap of 1 mm separating the source and the samples, has a negligible effect on the intensity of fission fragments emanating from the source and hitting sample surface. This is a good assumption since the reported range of fission fragments in air is about 23 mm,[32] making the air gap only about 4% of the range.

Although, as implied, the fission fragment production rate is uniform throughout the thickness of the source, only those formed within a small fraction of the total thickness are emitted from the surface of the source. This minimal thickness is termed the range of fission

fragments for any substance whether it be an absorber or emitter of these fragments. For the source employed in these experiments, 36 w/o of enriched UO_2 and balance stainless steel, the range, R_s, was approximated by the equation

$$\frac{1}{R_s} = \frac{1}{\text{Average Source Molecular Weight}} \left[\frac{55.9 \text{ (mol \% Fe)}}{100\ R_{Fe}} + \frac{267 \text{ (mol \% } UO_2)}{100\ R_{UO_2}} \right] \quad (C.1)$$

By interpolation of reported data,[28] it was found that R_{Fe} was 4.9 mg/cm^2 and R_{UO_2} was 11.9 mg/cm^2. The range of fission fragments in the source, R_s, was calculated to be 6.2 mg/cm^2 or 7.4 microns, assuming the average molecular weight of the source to be 78.0 and the density of the source to be 92% of theoretical or 8.35 g/cm^3.

To estimate the intensity of fission fragments being emitted, Holmes[31] has treated the source as an infinite slab with thickness x, measured from the exposed surface of the source. For any differential thickness, dx, the number of fission fragments produced is twice the number of fissions or $2\Sigma_f \phi dx$. The calculated macroscopic cross section for this source is 3.78 cm^{-1} while the neutron flux, ϕ, is that in the source.

Isotropic production of the fission fragments was assumed, so that the path taken by such particles originating at dx could be anywhere within a sphere whose radius is equivalent to the range of the source, R_s. The fraction of the total fragments that escaped from this surface can be expressed by the following ratio:

$$\frac{\text{Area of spherical cap of height h and radius } R_s}{\text{Total area of sphere of radius } R_s}$$

Schematically this is represented in Figure 17. Therefore the equation for I, the intensity of fission fragments hitting the zirconium surface, is

$$I = \int_{x=0}^{x=R_s} 2\Sigma_f \phi dx \; \frac{2\pi R_s h}{4\pi R_s^2} = \frac{2\Sigma_f \phi}{2 R_s} \int_{x=0}^{x=R_s} (R_s - x)\, dx$$

The integrated form of the above equation is

$$I = \frac{2\Sigma_f \phi \, R_s}{4} \qquad (C.2)$$

It is seen by equation (C.2) that 25% of those fragments formed within the range actually emerge from the surface of the source.

II. Estimation of the Range of Fission Fragments in Zirconium

The purpose in estimating the range of fission fragments in zirconium is to eventually estimate the fraction of the total number of zirconium atoms which were displaced during the period of each run within the volume of solid which essentially absorbs all of the fission fragments. This volume is equal to the product of the surface area exposed to fission fragment recoils and a thickness equivalent to the average range of the recoils in zirconium. The procedure by which this is done and its associated derivations are outlined below.

In order to estimate the range of fission fragments in zirconi-

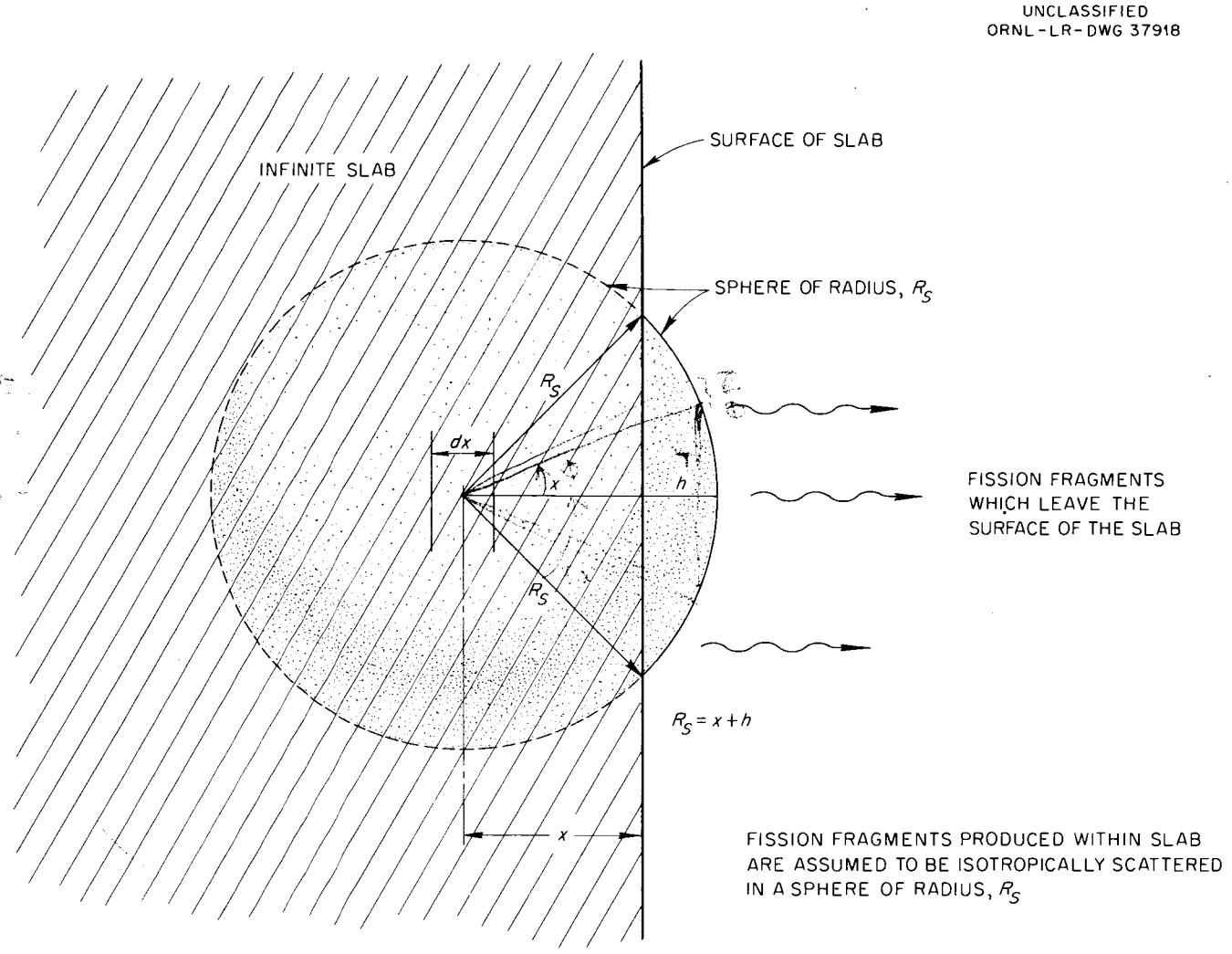

Fig. 17. Schematic Diagram Used for Derivation of Intensity of Fission Fragments Being Emitted at the Surface of an Infinite Slab.

um it is necessary to approximate the average energy of the fragments being emitted at the surface of the source. Only those fragments which are formed at and leave the surface of the source are of full energy. A portion of the energy of those fragments formed within the source and emitted at the surface, is absorbed within the source.

From Section I of this appendix it was assumed that the intensity of fission fragments hitting the zirconium is the same as that being emitted from the source and this was shown in equation (C.2) to be

$$I = \frac{2\Sigma_f \phi R_S}{4}$$

This equation also states, in effect, that the fragments coming out of the source embrace a whole spectrum of energies. This ranges from full energy, $E = E_o$, for those fragments formed and emitted at a path length, $r = 0$, at the surface of the slab (See Figure 17), to $E = 0$ for those fragments originating at a path length from the surface of the source equal to the range of fragments in the source, $r = R_S$, and reach the surface.

For the general case, $R_S \geq r \geq 0$, the intensity of fission fragments being emitted from the source surface having residual energies greater than E, is

$$I(E) = \frac{2\Sigma_f \phi \ r(E)}{4} \qquad (C.3)$$

where r(E) is the path length traversed by the fission fragment to the point at which it has energy E. The differential form of equation (C.3) is

$$dI(E) = \frac{2\Sigma_f \phi}{4} \ d\, r(E) \qquad (C.4)$$

Letting f(E) dE be the fraction of emerging particles which have energies

in dE, the expression for f(E) is

$$f(E) = \frac{\frac{dI(E)}{dE}}{\frac{2\Sigma_f \phi}{4} R_s}$$

By substitution, using equation (C.4), the expression becomes

$$f(E) = \frac{\frac{dr(E)}{dE}}{R_s}$$

Thus the average residual energy of a fission fragment emitted from the source and impinging on the zirconium specimen, $\bar{E}$, is

$$\bar{E} = \int_0^{E_o} Ef(E)\, dE = \int_0^{E_o} E \frac{\frac{dr(E)}{dE}}{R_s} dE$$

By changing variables, the simplified form of this expression is

$$\bar{E} = \frac{1}{R_s} \int_0^{R_s} E(r)\, dr \qquad (C.5)$$

where E(r) is the energy of the fission fragment after it has traversed a distance r.

Schmitt[33] has suggested that it is possible to normalize existing reported data[32] to obtain a very approximate general relationship between residual energy and range of the heavy and light fragments, respectively, in a solid. The curves are shown in Figure 18, and are the results of reported data of four elements ranging in atomic number from 13 to 79 — aluminum, argon, nickel and gold.[32]

Assuming that the 36 $^{w}/_{o}$ UO_2 - stainless steel fission fragment source has approximately the same normalized range to residual energy for both the heavy and light fragments as in Figure 18 and terming this

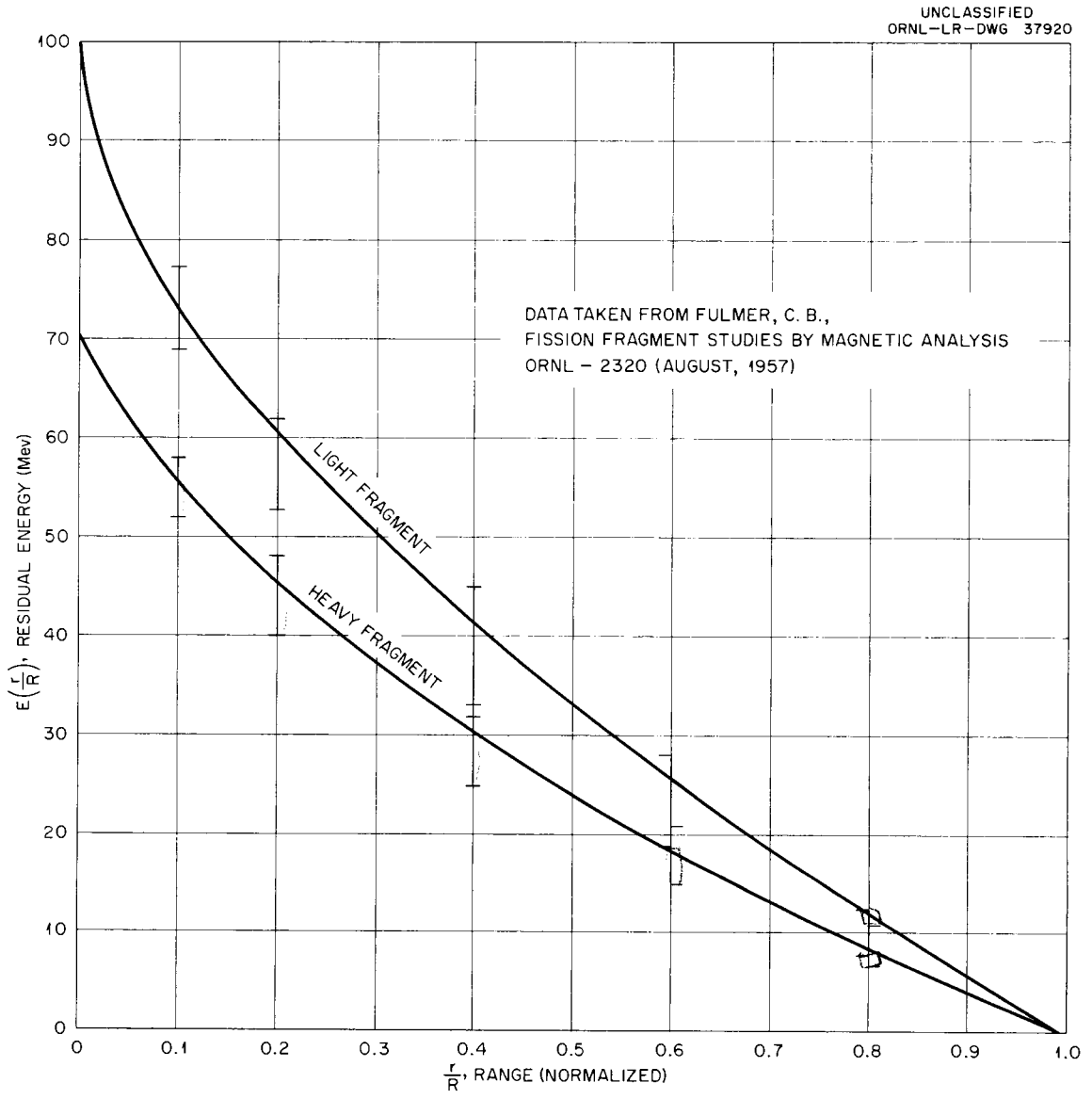

Fig. 18. Residual Energy of Fission Fragment vs Normalized Range of Fission Fragments in any Metal of Atomic Numbers 13 to 79.

assumed relationship as $\frac{r}{R_s}$ vs $E(\frac{r}{R_s})$, it is then possible to simplify equation (C.5) and it becomes

$$\bar{E} = \int_0^1 E(\frac{r}{R_s})\, d(\frac{r}{R_s}) \qquad (C.6)$$

Therefore the numerical integration of each of the two curves in Figure 18 will give the average energy, $\bar{E}$, for the light and heavy fragments respectively being emitted at the source and bombarding the zirconium specimen. Using this method, the estimated average energy of the light fragment being emitted from the source, $\bar{E}_L$, is found to be 37 Mev while that for the heavy fragment, $\bar{E}_H$, is 27 Mev. This indicates that only about 10% of the initial total energy of the fragments formed, within the range of fission fragments in the source, is actually emitted at the surface of the source.

By interpolating the reported data of Fulmer,[32] it is possible to get an estimated residual energy-range relationship for zirconium. This is shown in Figure 19. Using this figure to obtain the range of fission fragments in zirconium, it is seen that for the light fragment of $\bar{E}_L$ = 37 Mev, the corresponding range, R_L, is 4.1 mg/cm^2 and for the heavy fragment of $\bar{E}_H$ = 27 Mev, the corresponding range, R_H, is 3.2 mg/cm^2. Converting these values to thickness, R_L becomes 6.2 microns and R_H becomes 4.8 microns. The arithmetic average of these last two values is assumed to be the range of fission fragments in zirconium, namely, 5.5 microns.

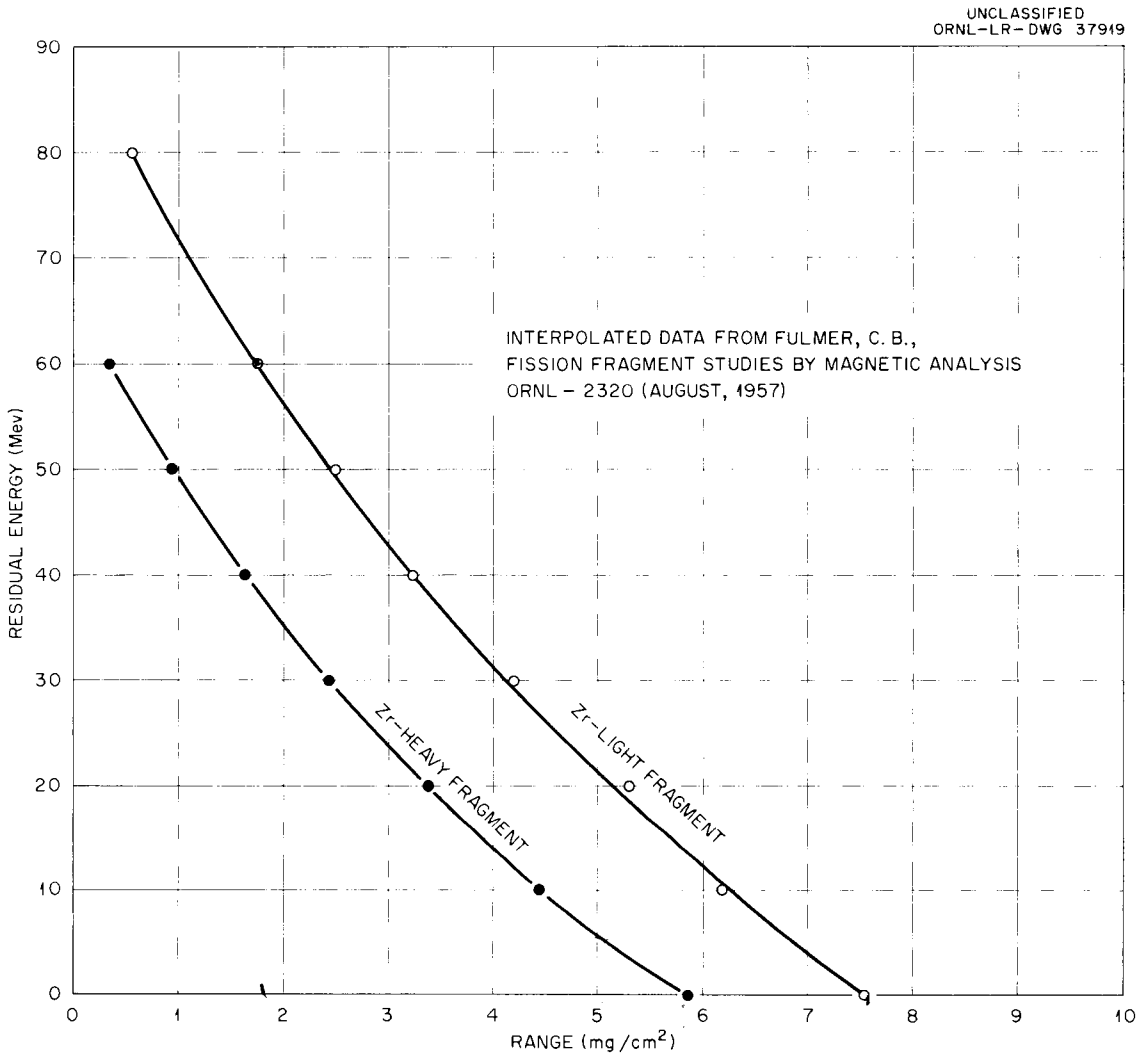

Fig. 19. Residual Energy of Fission Fragment vs Fission Fragment Range in Zirconium.

NOMENCLATURE

E	energy of fission fragment, Mev
$\bar{E}$	average energy of fission fragments, Mev
h	height of a spherical cap, microns
I	intensity of fission fragments, particles/cm^2/second
N	number of active nuclei
R	range of fission fragment, cm, microns, or mg/cm^2
r	path length of fission fragment, cm or microns
T	irradiation time, seconds
t	decay time, seconds
$t_{\frac{1}{2}}$	half-life, days
V	volume of absorber, cm^3
x	thickness of fission fragment recoil source, microns
w/o	weight percent
a/o	atom percent
ϕ	thermal neutron flux, neutrons/cm^2/second
Σ_a	macroscopic absorption cross section, cm^{-1}
Σ_f	macroscopic fission cross section, cm^{-1}
λ	radioactive decay constant, $seconds^{-1}$

Superscripts

1	irradiation period
2	decay period

Subscripts

H heavy fission fragment

L light fission fragment

s fission fragment recoil source

1 Zr^{95}

2 Nb^{95}

ORNL-2742
UC-40 Radiation Effects on Materials
TID-4500 (15th ed.)

INTERNAL DISTRIBUTION

1. HRP Director's Office Rm. 259, Bldg. 9204-1
2. G. M. Adamson
3. A. L. Bacarella
4. J. E. Baker
5. J. C. Banter
6. S. E. Beall
7. R. J. Beaver
8. D. S. Billington
9. R. E. Blanco
10. E. P. Blizard
11. J. O. Blomeke
12. E. G. Bohlmann
13. C. D. Bopp
14. C. J. Borkowski
15. D. T. Bourgette
16. C. M. Boyd
17. G. E. Boyd
18. J. W. Boyle, Jr.
19. J. C. Bresee
20. W. H. Bridges
21. F. R. Bruce
22. C. D. Cagle
23. G. H. Cartledge
24. W. L. Carter
25. W. R. Casto
26. J. V. Cathcart
27. C. E. Center
28. R. A. Charpie
29. W. E. Clark
30. R. S. Cockreham
31. E. L. Compere
32. J. H. Crawford
33. F. L. Culler
34. J. E. Cunningham
35. R. J. Davis
36. L. M. Doney
37. A. C. Downing
38. L. B. Emlet (K-25)
39. J. L. English
40. D. E. Ferguson
41. J. H. Frye, Jr.
42. C. B. Fulmer
43. W. R. Gall
44. H. W. Godbee
45. R. J. Gray
46. W. R. Grimes
47. J. P. Hammond
48. W. O. Harms (consultant)
49. W. W. Harris (K-25)
50. P. N. Haubenreich
51. C. J. Hochanadel
52. E. E. Hoffman
53. D. L. Holcomb
54. R. R. Holcomb
55. D. K. Holmes
56. A. S. Householder
57. G. H. Jenks
58. L. K. Jetter
59. D. T. Jones
60. W. H. Jordan
61. P. R. Kasten
62. G. W. Keilholtz
63. C. P. Keim
64. M. T. Kelley
65. J. A. Lane
66. C. F. Leitten
67. S. C. Lind
68. R. S. Livingston
69. E. L. Long, Jr.
70. M. I. Lundin
71. T. S. Lundy
72. R. N. Lyon
73. W. D. Manly
74. R. E. McDonald
75. H. F. McDuffie
76. C. J. McHargue
77. J. R. McWherter
78. R. E. Meyer
79. A. J. Miller
80. K. Z. Morgan
81. J. P. Murray (Y-12)
82. M. L. Nelson
83. T. S. Noggle
84. A. R. Olsen
85. G. W. Parker
86. W. W. Parkinson, Jr.
87. P. Patriarca
88. S. W. Peterson
89. M. L. Picklesimer
90. F. A. Posey
91. S. A. Reed
92. P. M. Reyling
93. D. M. Richardson

94. J. T. Roberts
95. P. S. Rudolph
96. H. C. Savage
97. H. W. Schmitt
98. H. E. Seagren
99. C. H. Secoy
100. F. A. Sherrill
101. E. D. Shipley
102. M. D. Silverman
103. O. Sisman
104. M. J. Skinner
105. G. M. Slaughter
106. C. O. Smith
107. G. P. Smith, Jr.
108. A. H. Snell
109. B. A. Soldano
110-115. E. E. Stansbury (consultant)
116. J. A. Swartout
117. W. H. Tabor
118. A. J. Taylor
119. E. H. Taylor
120. W. C. Waggener
121. A. M. Weinberg
122. M. E. Whatley
123. T. E. Willmarth
124. C. E. Winters
125. M. C. Wittels
126. L. F. Woo
127. R. G. Wymer
128. H. L. Yakel, Jr.
129-148. W. C. Yee
149. F. W. Young
150. Biology Library
151-152. Central Research Library
153. Chemistry Division Files
154. Health Physics Library
155-164. Laboratory Records Department
165. Laboratory Records, ORNL R.C.
166. Metallurgy Library
167. Reactor Experimental Engineering Library
168. ORNL - Y-12 Technical Library

EXTERNAL DISTRIBUTION

169. Division of Research and Development, AEC, ORO
170. D. H. Groelsema, AEC, Washington
171. J. E. Draley, ANL
172. F. L. Yagee, ANL
173. H. A. Fisch, KAPL
174. J. T. Waber, LASL
175. S. Isserow, NMI
176. J. P. Pemsler, NMI
177. Dow Chemical Company (Rocky Flats)
178. Grand Junction Operations Office
179. M and C Nuclear, Inc.
180-181. National Lead Company of Ohio
182. New Brunswick Area Office
183. Olin Mathieson Chemical Corporation
184. Stevens Institute of Technology (Comstock)
185. U.S. Geological Survey, Menlo Park
186-764. Given distribution as shown in TID-4500 (15th ed.) under Radiation Effects on Materials (75 copies - OTS)